

PETROLOGY AND MOLYBDENITE MINERALIZATION  
OF  
THE LUCKY SHIP IGNEOUS COMPLEX

803177 BY David A. Silversides

PETROLOGY AND MOLYBDENITE MINERALIZATION

OF

THE LUCKY SHIP IGNEOUS COMPLEX

932/4

---

A Thesis

Presented to

the Department of Geology

The University of Manitoba

---

In Partial Fulfillment

of the Requirements for the Degree

Master of Science

---

by

David A. Silversides

January 1968

## ABSTRACT

The Lucky Ship Property is located in west-central British Columbia. Molybdenite mineralization occurs in a stockwork of quartz veinlets spatially associated with an igneous complex intruding Jurassic sediments assigned to the Hazelton Group.

Five distinct rock types make up the complex: pink quartz porphyry, grey biotite-quartz-feldspar porphyry, dark green aphanitic dykes, white quartz-feldspar porphyry, and alaskite. On the basis of chemical analyses, these correspond to very potash-rich granite, quartz monzonite, lamprophyre, and alkali granite.

The white quartz-feldspar porphyry and the alaskite, both alkali granites, have a common composition of albitic plagioclase,  $Ab_{98-92} An_{2-8}$ . It is concluded they are related. The albite has optical properties implying crystallization under plutonic conditions.

Potash metasomatism, indicated mineralogically by sericite and potash feldspar as a replacement of the albite, and chemically by a marked increase in  $K_2O$ , has been extensive in the white quartz-feldspar porphyry and the alaskite.

Inconclusive evidence suggests that white quartz-feldspar porphyry is younger than grey biotite-quartz-feldspar porphyry.

Molybdenite mineralization is associated with the crystallization history of the white-quartz-feldspar porphyry. This is indicated by the presence of mineralized fragments included in this rock, which itself is cut by a second period of mineralization.

## TABLE OF CONTENTS

ABSTRACT . . . . .	iii
CHAPTER	PAGE
I. INTRODUCTION . . . . .	1
Statement of Problem . . . . .	1
Location and Access . . . . .	1
History . . . . .	3
Acknowledgments . . . . .	4
II. GENERAL GEOLOGY . . . . .	5
Regional Geologic Setting . . . . .	5
Local Setting . . . . .	9
General Geology of the Igneous Complex . . . . .	10
III. IGNEOUS ROCK UNITS . . . . .	15
Petrology . . . . .	15
(i) Pink Quartz Porphyry . . . . .	15
(ii) Grey Biotite-Quartz-Feldspar Porphyry . . . . .	16
(iii) Dark Green Aphanitic Dykes . . . . .	22
(iv) White Quartz-Feldspar Porphyry . . . . .	24
(a) Plagioclase feldspar . . . . .	30
(b) Potash feldspar . . . . .	33
(v) Alaskite Dykes . . . . .	40
Chemical Analyses and Classification of the Igneous Rock Units of the Complex . . . . .	44
(i) Pink Quartz Porphyry . . . . .	44
(ii) Grey Biotite-Quartz-Feldspar Porphyry . . . . .	44



CHAPTER	PAGE
(iii) Dark Green Aphanitic Dykes . . . . .	46
(iv) White Quartz-Feldspar Porphyry . . . . .	46
(v) Alaskite Dykes . . . . .	47
IV. MOLYBDENITE MINERALIZATION AND HYDROTHERMAL ALTERATION . . . . .	51
Molybdenite Mineralization . . . . .	51
Hydrothermal Alteration . . . . .	54
(i) Sericitization . . . . .	55
(ii) Potash Feldspathization . . . . .	55
(iii) Argillization . . . . .	56
(iv) Saussuritization . . . . .	62
(v) Pyritization . . . . .	62
V. INTERPRETATION AND CONCLUSIONS . . . . .	68
Environment of the Igneous Rock Types . . . . .	68
The Relative Ages of White Quartz-Feldspar Porphyry and Grey Biotite-Quartz-Feldspar Porphyry and the Genesis of Molybdenite Mineralization . . . . .	71
Conclusions . . . . .	78
REFERENCES . . . . .	80
APPENDIX . . . . .	83

## LIST OF FIGURES

FIGURE	PAGE
1. Location of the Lucky Ship Property . . . . .	2
2. Regional Geology . . . . .	6
3. Legend for Figures 4, 6, and 7 . . . . .	back pocket
4. Surface Geology . . . . .	back pocket
5. Poles to Bedding Planes in Argillites . . . . .	11
6. Diamond Drill-hole Cross-sections . . . . .	back pocket
7. Location of Thin-sections and Chemical Analyses . . . . .	back pocket
8. Contour Diagram of Poles to Joints in White Quartz-Feldspar Porphyry . . . . .	25
9. Universal Stage Orientation and Derivation of $X\wedge TA$ and $Y\wedge TA$ for Two Adjacent Albite Twin Lamellae in Plagioclase . . . . .	32
10. Twinning-axis Curves for the Albite Twin Law . . . . .	34
11. $2V_z$ Values for Plutonic and "High Temperature" Plagioclases . . . . .	34
12. Universal Stage Orientation of Baveno Twin, Potash Feldspar Phenocryst . . . . .	36
13. Triangular Diagram of Weight % of $K_2O$ , $Na_2O$ , and $CaO$ from Analyses of Table V . . . . .	48

FIGURE	PAGE
14. Schematic Crystallization of the System	
Albite-Anorthite-Orthoclase, Showing the Derivation of White Quartz-Feldspar Porphyry	
(after Barth, 1962) . . . . .	73

## LIST OF TABLES

TABLE	PAGE
I. Modal Analyses of Grey Biotite-Quartz- Feldspar Porphyry . . . . .	21
II. Modal Analyses of White Quartz-Feldspar Porphyry . . . . .	28
III. $2V_z$ , $X_{ATA}$ and $Y_{ATA}$ of Albite-Twinned Plagioclase in White Quartz-Feldspar Porphyry . . . . .	33
IV. $2V$ Values and Extinction Angles on (010) for Potash Feldspar Phenocrysts . . . . .	35
V. Chemical Analyses of Igneous Rock Types . . . . .	45
VI. Comparative Analyses From Nockolds (1954) . . . . .	45
VII. C.I.P.W. Normative Minerals of the Four Porphyry Rock Units . . . . .	49

## LIST OF PHOTOGRAPHS

PLATE	PAGE
1. Pink quartz porphyry . . . . .	17
2. Outcrop of grey biotite-quartz-feldspar porphyry with abundant quartz veins . . . . .	20
3. Photomicrograph of least altered grey biotite- quartz-feldspar porphyry . . . . .	20
4. Dark green aphanitic dyke unit . . . . .	23
5. White quartz-feldspar porphyry . . . . .	29
6. Quartz-veined fragment of white quartz-feldspar porphyry surrounded by white quartz-feldspar porphyry . . . . .	38
7. Possible inclusion of dark green aphanitic dyke unit in breccia portion of white quartz- feldspar porphyry . . . . .	39
8. Cataclastic structure in breccia portion of white quartz-feldspar porphyry . . . . .	41
9. Alaskite dyke unit . . . . .	43
10. Potash feldspar replacement of plagioclase . . . . .	57
11. Potash feldspar replacement of plagioclase . . . . .	58
12. Argillization of white quartz-feldspar porphyry . . . . .	60
13. Argillization of plagioclase phenocrysts in grey biotite-quartz-feldspar porphyry . . . . .	61

PLATE	PAGE
14. Saussuritization of plagioclase phenocrysts	
in white quartz-feldspar porphyry . . . . .	63
15. Abundant quartz veins in white quartz-	
feldspar porphyry . . . . .	66

## CHAPTER I

### INTRODUCTION

#### Statement of Problem

The Lucky Ship Property is a molybdenite prospect in a complex of fine-grained, igneous porphyries. The writer's objectives in this study are:

(i) To describe the porphyry types as to their known and implied distribution, petrography, alteration, chemical variation, and petrogenesis.

(ii) To give an account of the molybdenite mineralization with regard to its distribution and possible origin in the complex.

#### Location and Access

The Lucky Ship Property is situated between Morice Lake and the Nanika River in west-central British Columbia (fig. 1). The small village of Houston, approximately 50 miles northeast of the property, is the nearest supply center. Access is easily obtained via the Morice Lake Forestry Development Road from Houston up to mile 49 on the east side of the Nanika River, thence via a connecting road, six miles in length, to the property's camp site.



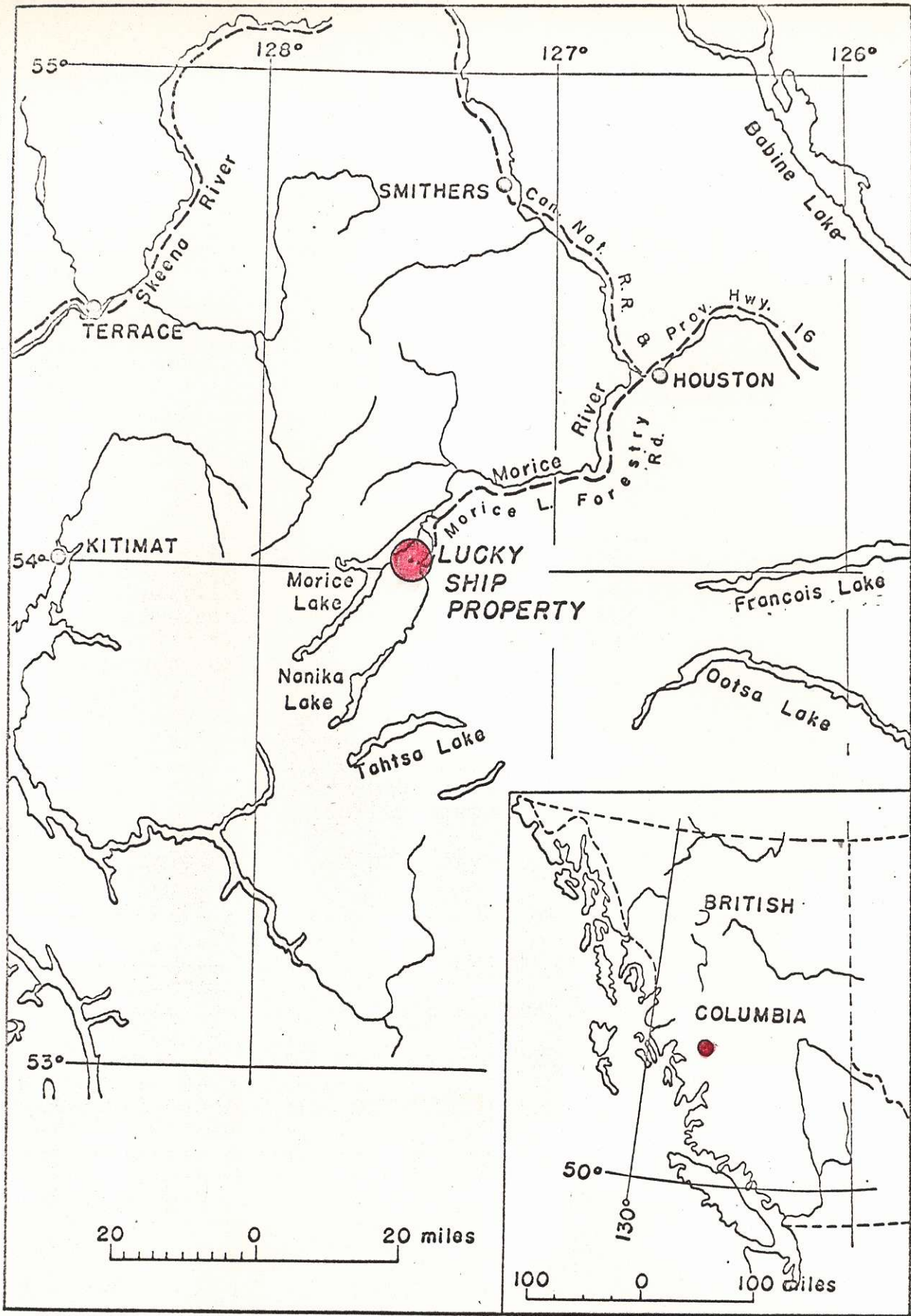


Fig. 1 - Location of the Lucky Ship Property

History

The area which includes the Lucky Ship Property has been mapped in reconnaissance fashion by Armstrong (1944), but no description of the property is given in his report. To the writer's knowledge, the only mention of the property in published literature is that contained in the 1957 British Columbia Department of Mines Report:

"Lucky Ship (54° 127° SW)

This property consists of fifteen recorded claims, owned by Matthew Sam and B. McCrae of Topley;..... It covers a zone of quartz stringers containing molybdenite that cut quartz porphyry. The Consolidated Mining and Smelting Company of Canada, Limited, optioned the property and in July, 1957 did 203 lineal feet of trenching."

Apparently the property was dropped by the above company in the fall of 1957 and returned to the vendors. In the spring of 1963, the property was optioned by Plateau Minerals Limited who conducted a geochemical soil survey and staked additional claims. Southwest Potash Corporation, in turn, optioned the property from Plateau Minerals in September 1963 and proceeded to stake additional claims, cut picket lines, and conduct mapping, geochemical soil surveys, and magnetometer surveys during September, October, and November.

During the period June-November, 1964, Southwest

Potash Corporation undertook a more ambitious development programme consisting of prospecting the entire claim group, (which now consists of approximately 109 claims), detailed mapping of the mineralized area, and diamond drilling four holes totalling 4246 lineal feet.

The writer collected most of the material for this paper during the period of June to mid-September, 1964 while employed by Southwest Potash Corporation to do the detailed mapping. Drill logs and representative core from the last three holes which were completed after the writer left the property, were obtained in December, 1964. Thin-section studies, determination of minerals by x-ray methods, and library research was conducted during the 1964-1965 winter term at the University of Manitoba.

#### Acknowledgments

The writer wishes to acknowledge the authorities of Southwest Potash Corporation who kindly granted permission to use the geologic data of the Lucky Ship Property for this thesis. Professors G. M. Brownell, W. C. Brisbin, and A. C. Turnock of the University of Manitoba, and I. Haugh of the Manitoba Department of Mines, gave constructive and appreciated criticisms of the manuscript.

## CHAPTER II

### GENERAL GEOLOGY

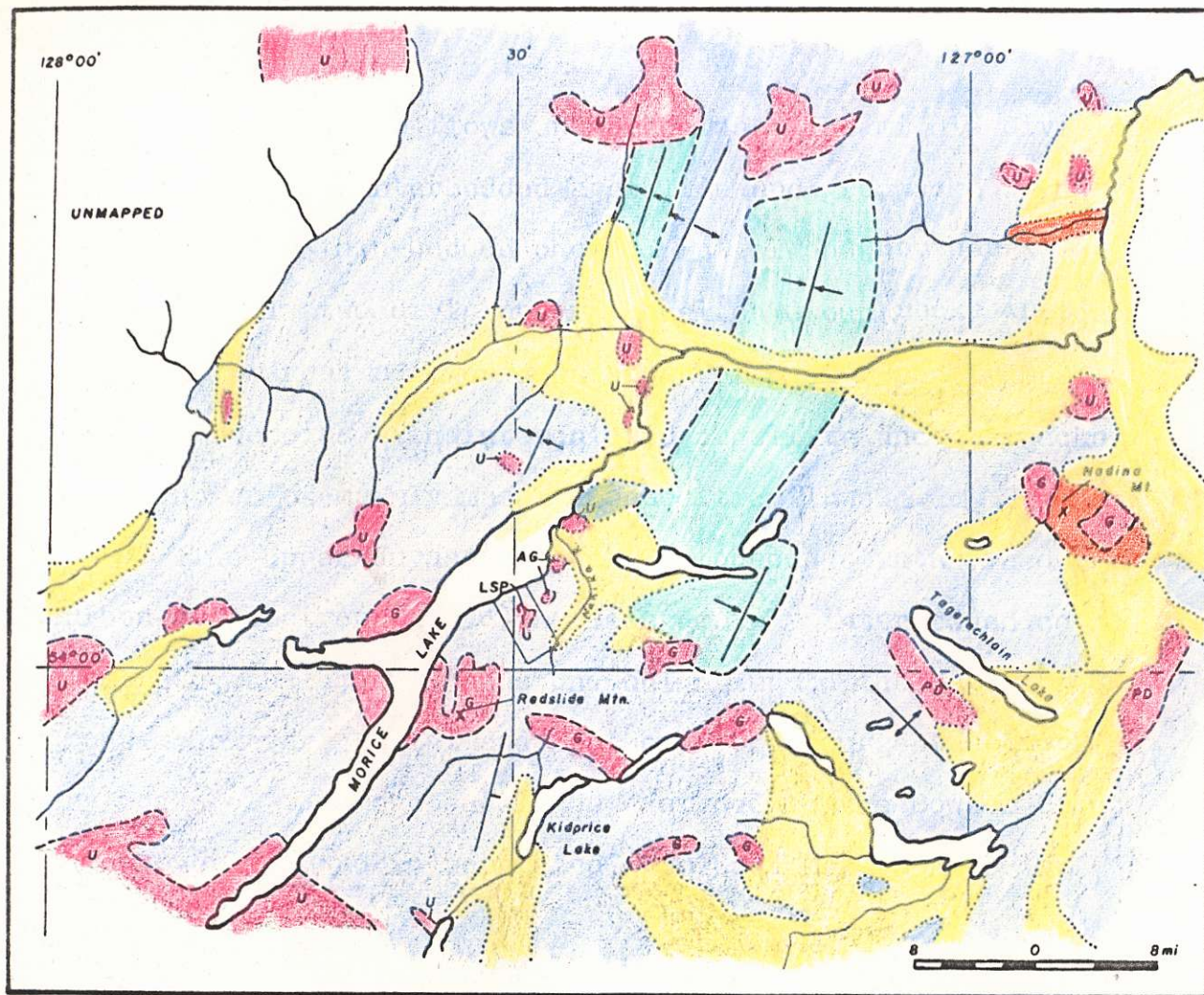
#### Regional Geologic Setting

Figure 2, compiled from the maps of Armstrong (1944), Duffel (1959), Lang (1942), and Rice (1949), depicts the regional geologic setting of the property. The following description is basically a summary of their work in this area and that of Duffel and Souther (1964), whose recent work in the Terrace Map Area immediately east of figure 2, adds considerably to the understanding of the igneous geology of the Coast Range.

The property lies east of the major batholiths of the Coast Range, within an area containing numerous small granitic plutons. The small plutons intrude Hazelton Group (Jurassic) rocks, to some extent strata of the Bowser Group (Upper Jurassic to Lower Cretaceous), and rocks of the Sustut Group (Upper Cretaceous and Paleocene).

The Hazelton Group consists of an apparently conformable succession of interbedded volcanic and sedimentary rocks which has been divided by Duffel (1957) into a lower mainly volcanic division, a middle mainly sedimentary division, and an upper dominantly volcanic division. The lower and upper divisions are characterized by a larger proportion of





**LEGEND**

- Pleistocene  Gravel, till.
- Upper Cretaceous-  
Paleocene  Sustut Group: conglomerate, sandstone, shale, greywacke, argillite.
- Lower Jurassic-  
Early Tertiary  Coast Intrusions: undifferentiated(U), granite(G), aplitic granite(AC), porphyritic diorite(PD), Lucky Ship porphyries(LSP).
- Upper Jurassic-  
Lower Cretaceous  Bowser Group: conglomerate, shale, sandstone.
- Jurassic  Hazelton Group: andesite, basalt, argillite, greywacke.
- Lucky Ship Property.

**REGIONAL GEOLOGY**

Fig. 2

porphyritic andesite flows and breccias. The middle division is predominantly interbedded argillite and greywacke with minor tuff and thin-bedded chert. Duffel and Souther (1964) recognize only two divisions in Hazelton Group rocks in the Terrace Map Area; a lower consisting of predominantly massive andesite breccias with intercalated argillite and greywacke and an upper of mainly massive andesitic flows.

The Upper Jurassic-Lower Cretaceous strata are described by Armstrong (1944) as being mainly interbedded conglomerate, shale, and sandstone belonging to the Hazelton Group. However, Duffel and Souther (1964) suggest sedimentary rocks of this age should be assigned to the Bowser Group which overlies and is separated from Hazelton rocks by an unconformity.

The Upper Cretaceous strata are described by Lang (1942) as being mainly sandstone, greywacke, and conglomerate. Rice (1949) correlates these rocks to the Sustut Group of Upper Cretaceous and Paleocene age in his compilation of the Smithers-Fort St. James sheet.

Structurally, the Hazelton Group and Bowser Group rocks are depicted as being folded into a series of northeasterly trending synclines and anticlines. This feature is a departure from the general northwesterly trend of folding present in rocks adjacent to the Coast Range batholithic

complex.

The plutons shown in figure 2 consist of a granitic suite collectively described in the literature as being granodiorite, quartz diorite, diorite, granite, and related rocks. Together with the major batholithic rocks of the largely granitic terrain of the Coast Range proper, they are grouped under the classification of Coast Intrusions (Duffel, 1959; Duffel and Souther, 1964). Their emplacement ranges over a period of possibly Lower Jurassic to early Tertiary, with perhaps the majority emplaced during the Cretaceous period (Duffel, 1959).

Very few of the individual plutons are described in terms of specific rock type. Lang (1942) states that the granitic stock of Nadina Mountain is a red granite; elsewhere the intrusions are classified as granite and diorite. Armstrong (1944) does not describe any individual pluton. Duffel (1959) is the most precise calling the intrusion at Redslide Mountain granite; those northeast of Kidprice Lake granite, and those in the vicinity of Tagetochlain Lake porphyritic diorites. The intrusive rock at the south end of Morice Lake is an apophysis extending eastward from the main batholithic complex and is not described as to specific rock type in the literature. However, Souther's work (Duffel and Souther, 1964) on similar apophyses in the Terrace Map



Sheet indicates that it is most likely a complex of rock types ranging from granite to gabbro, with the bulk being granodioritic in composition.

#### Local Setting

The Lucky Ship Property covers an area of approximately 5 square miles situated astride the heavily wooded ridge between Morice Lake and the Nanika River. The slopes of the ridge are steep, rising from an elevation of approximately 2600 feet at the base to 4400 feet at the crest. The terrain is rugged with numerous bluffs.

The ridge is largely underlain by volcanic rocks and to a lesser extent by sedimentary rocks of the Hazelton Group. These have been intruded by several small plutons and dykes. Overburden consisting of glacial till and gravel is fairly extensive, particularly at elevations below 3500 feet.

The volcanic rocks comprising the Hazelton Group are dark green to red andesites, tuffs, agglomerates, and black to red amygdaloidal basalts. The sedimentary rocks are argillite, greywacke, and greywacke conglomerate. Their predominant strike direction is believed to be north-north-east, with dips to the southeast.

The plutons and dykes include two small (less than 2000 feet in diameter), aplitic granite stocks, several

quartz porphyry and felsite dykes, and a complex containing a variety of fine-grained porphyries and dark green aphanitic dykes. This latter complex is the most significant feature of the area because of its associated molybdenite mineralization. The general geology of this complex is described in the following section

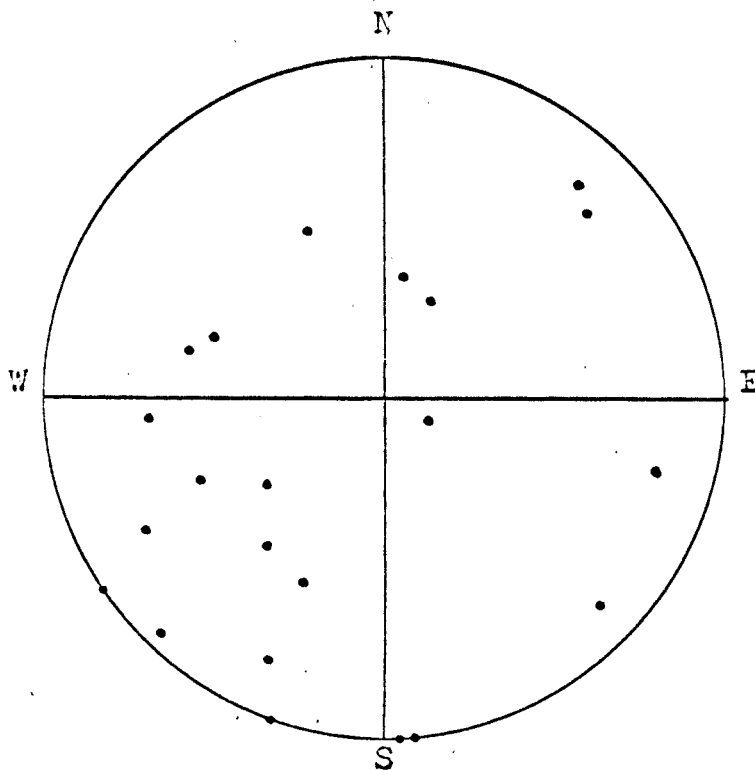
#### General Geology of the Igneous Porphyries

Figures 3, 4, and 6 (included in back pocket) refer to surface geology and diamond drill-hole sections.

The surface geology of the complex is shown in fig. 4. The igneous rock types of the complex form a highly irregular shaped mass located at the crest and on the south-east slopes of the ridge between the elevations of 3200 and 4300 feet. The dimensions of the complex are approximately 4000 feet in a N-S direction and 2500 feet in an E-W direction.

The host rocks for the igneous rock types of the complex are interbedded cherty argillites, argillites, greywackes, and greywacke conglomerates. Argillites predominate in the eastern half of the map-area of fig. 4; greywacke and greywacke conglomerate predominates in the western half. No obvious andesite flows were observed, but the majority of the rock fragments in the greywackes are andesite.

Lateral and vertical gradational variations in the sedimentary rock types are very common and make it difficult to determine bedding planes. Distinct bedding planes are most frequently observed in the argillites, but the few observations recorded do not fall into any set pattern (see fig. 5). The only interpretation that can be made from these few measurements is that the rocks are folded and dips are generally greater than  $40^{\circ}$ .



- 22 attitudes plotted from field observations.
- lower hemisphere stereographic projection.

Fig. 5 - Poles to bedding planes in argillites

The igneous complex consists of fine-grained silicic porphyries and dark green aphanitic dykes. The rock types fall into five mappable units on the basis of megascopic appearance:

(i) Pink quartz porphyry. This rock type is light red and contains 2 to 3 per cent glassy quartz phenocrysts 0.5 to 1 mm in diameter and minor disseminated flakes of specular hematite. The matrix is light red in colour and exceedingly fine-grained.

(ii) White quartz-feldspar porphyry. The megascopic appearance of this rock type is variable due to alteration and differences in the amount of phenocrysts. Its most characteristic feature is its brilliant white color. The phenocrysts are quartz, feldspars, and biotite, ranging from 0.1 to 4.0 mm in diameter. Quartz phenocrysts are always visible. The biotite content varies from nil to approximately 1 per cent. The feldspars are generally visible, but in some instances blend in with the white colored matrix or are masked by alteration. Alteration minerals visibly recognized are fine-grained sericite, "clay", epidote, and pyrite.

White quartz-feldspar porphyry also contains angular, light to dark colored fragments. The dark fragments are visibly recognized as inclusions of the surrounding sedimentary rocks. The abundance of the fragments varies from nil

to approximately 40 per cent of the total rock volume. Where concentrations are high, outcrops take on a breccia appearance.

(iii) Alaskite dykes. These dykes appear to be equigranular in handspecimens and are light green to cream in color. They are composed of 2 to 4 mm quartz and feldspar crystals. The dykes contain abundant quartz-molybdenite veinlets.

(iv) Dark green aphanitic dykes. Dykes of this rock type are dark green in color and very fine-grained. They contain disseminated pyrite and are cut by carbonate shears.

(v) Grey biotite-quartz-feldspar porphyry. This is a medium-grey colored rock containing visible biotite, white plagioclase, and glassy quartz phenocrysts set in a light grey, aphanitic matrix. The phenocrysts are 0.1 to 4 mm in diameter.

In the above classification, the term "porphyry" is used in the same sense as defined by Tyrell (1926):

" A porphyry is a hypabyssal form of plutonic magma, exhibiting one or more of the phenocrysts in an aphanitic groundmass."

The term is therefore used in a genetic as well as a textural sense.

The major problem encountered in mapping (see fig. 4) was the difficulty in establishing the boundaries of the

above igneous rock units. The reasons for this are:

- (i) A general lack of outcrop.
- (ii) Relatively intense alteration and quartz-veining, particularly in the southern portion of the complex, masks the true character of the rock units. Consequently, in many areas only the approximate position of the boundaries between rock types could be determined.

The white quartz-feldspar porphyry is the major rock type in the complex in terms of volume. Grey biotite-quartz-feldspar porphyry appears to be restricted to the southeastern portion of the complex. The dark green aphanitic dykes were discovered only in drill-core (see fig. 6, back pocket). The alaskite dykes were found only in the sedimentary host rock at the south contact of the complex. The pink quartz porphyry occurs at the western part of the complex.

The greatest intensity of fracturing, quartz veining, and alteration occurs in the south part of the complex. Molybdenite occurs as very fine-grained flakes in the quartz veinlets.

In the following chapter, descriptions of igneous rock types, alteration, and molybdenite mineralization are given with reference to petrology, geochemistry and mineralogy.

## CHAPTER III

### IGNEOUS ROCK UNITS

The unaltered or least altered igneous rock units of the complex are described. References to particular thin-section and chemically analyzed specimens have been made in the descriptions. Locations of specimens from outcrops are shown in fig. 7 (in back pocket). The locations of drill-core specimens are given in the text of the descriptions.

#### Petrology

##### (i) Pink Quartz Porphyry

This rock type occurs in the west portion of the complex (see fig. 4). Its outcrop distribution suggests a northwest trending body with an apparent width of 500 feet. Its contact with sedimentary rocks, observed in only one locale, was determined to have an attitude of  $320^{\circ}/90^{\circ}$ . Its contact relationship with white quartz-feldspar porphyry is unknown.

The rock is highly fractured and sheared. One predominant set of fractures trends northwest and dips vertically.

The most characteristic feature of the pink quartz porphyry is that it contains fine-grained (0.5 to 1 mm), disseminated flakes of specular hematite. This mineral was



also observed in the sedimentary rocks in contact areas. Glassy quartz phenocrysts are rare. The rock, in general, has a pink, porcelaneous appearance.

In thin-section, (see plate 1) the matrix appears as a very fine-grained ( $< 0.05$  mm) mixture of sericite, feldspar, and quartz. The quartz phenocrysts appear as subhedral crystals ranging from 0.5 to 2 mm in diameter. Potash feldspar occurs as anhedral and subhedral crystals, with specular hematite and sericite in the centers.

In the one observed contact area (see fig. 4, northern contact), the sedimentary argillite rocks are slightly metamorphosed to a dark green, epidote-chlorite hornfels. This feature indicates the pink quartz porphyry is intrusive.

(ii) Grey Biotite-Quartz-Feldspar Porphyry

Observed surface exposures of this rock unit generally contain a high frequency of quartz veinlets and are altered to a white aplitic mixture of quartz, "sericite", and "clay" which makes altered equivalents of this rock unit easily confused with the highly quartz-veined white-quartz-feldspar porphyry (see plate 2). Consequently, its boundaries shown on fig. 4 are uncertain and should be regarded as only approximate. The surface distribution of this rock type was based on the occurrence of remnant biotite (and/or chlorite), which is a characteristic mineral of unaltered



X 37, crossed nicols

Photomicrograph of pink quartz porphyry showing partially resorbed quartz phenocrysts (Q), potash feldspar (K), and specular hematite (H), set in a matrix of quartz, feldspar, and sericite. Taken from thin-section L.S.-53, outcrop.

Plate 1 - Pink Quartz Porphyry.

segments of this rock type. In drill-core, the two rock types are easier to determine. Altered grey biotite-quartz-feldspar porphyry is a dark green color, due to its relatively high chlorite content. Altered white quartz-feldspar porphyry is a very pale green color.

The suggested surface configuration is that of an oval-shaped body, approximately 800 feet long in a northeasterly direction and with a maximum width of 450 feet. One five foot thick dyke of this rock unit, having an attitude of  $N 30^{\circ} E/90^{\circ}$ , outcrops in sedimentary rocks south of the main body and was intersected in drill-holes 1 and 3.

The subsurface distribution of this rock unit, interpreted from an examination of drill core, is shown in fig. 6. Drill-hole 4 encountered no grey biotite-quartz-feldspar porphyry and therefore confirms the approximate northeastern termination as suggested from surface geology. Drill-hole 3 intersected alternate sections of grey biotite-quartz-feldspar porphyry, argillite and greywacke, and white quartz-feldspar porphyry. Drill-holes 1 and 2 cut through the maximum width of the body and subsequently contain the largest intersections. The projection of intersections in drill-core to surface indicates that the dip of the contacts of this rock unit are probably steep,  $70^{\circ}$  to vertical, and variable in direction.

The least altered portions of this rock unit contain

megascopically recognizable white feldspar, black biotite, and glassy quartz phenocrysts, set in a medium grey, aphanitic matrix.

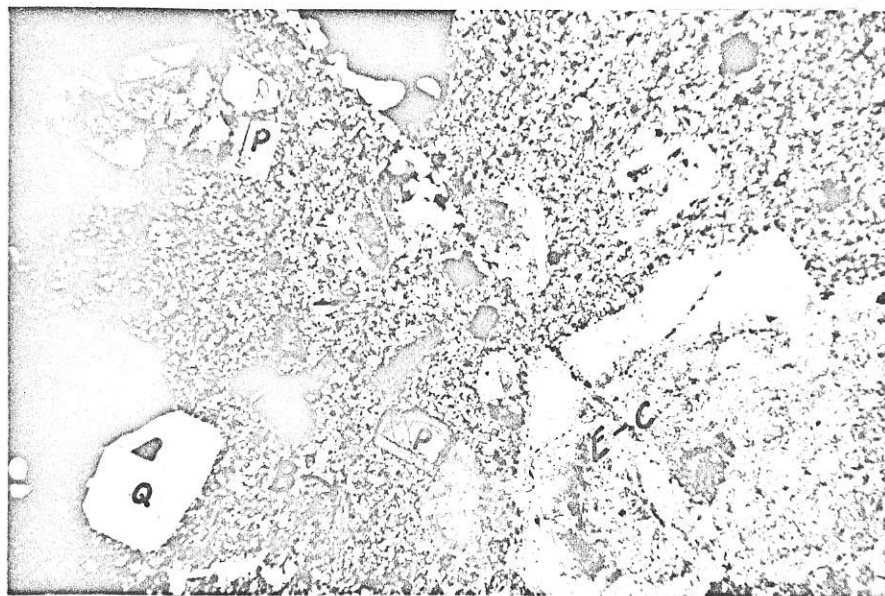
Under the microscope (see plate 3), the matrix appears as a very fine-grained ( $< 0.05$  mm) aggregate of quartz and both potash and plagioclase feldspars. Quartz phenocrysts occur as euhedral to subhedral, partially embayed crystals. Biotite appears as dark to light brown pleochroic flakes, partially altered to light green chlorite containing yellowish brown needles of rutile and fine-grained, earthy aggregates of leucoxene. The feldspar phenocrysts are plagioclase, showing strong normal zoning from andesine (approx.  $An_{35}$ ) in the centers to oligoclase (approx  $An_{25}$ ) at the rims. Phenocrysts of the above minerals range from 0.1 to 4 mm in diameter and average 1.0 mm. Trace amounts of apatite, closely associated with biotite, appears <sup>as</sup> the only recognizable accessory mineral.

The plagioclase phenocrysts show incipient alteration to fine-grained epidote and carbonate in the more calcic centers. This, and the weak chloritic alteration of biotite, likely represents deuteric reaction during final stages of crystallization. Where the rock is cut by numerous quartz veins, the plagioclase phenocrysts are completely altered to olive green, "clay" pseudomorphs.

Modal analyses of five specimens of grey quartz-feldspar porphyry are shown in Table I and were derived by the



Plate 2 - Outcrop of grey biotite-quartz-feldspar porphyry, with abundant quartz veins.



X 20, crossed nicols

- Q = quartz
- P = plagioclase
- B = biotite
- E-C = epidote-carbonate

Plate 3 - Photomicrograph of least altered grey biotite-quartz-feldspar porphyry.

point count method (Chayes, 1949). For each section at least 2000 points were counted, using an intercept distance of 0.3 mm and a traverse spacing of 0.5 mm. If a hole occurred during a traverse, the counting was stopped and a new traverse begun. Only phenocrysts are distinguished in their mineralogy; the minerals occurring in the matrix are too fine-grained to accurately determine their identity.

Table I

Modal Analyses of Grey Biotite-Quartz-Feldspar Porphyry

Specimen Number	Volume %				
	Matrix	Plagioclase	Quartz	Biotite Chlorite	Apatite
L.S.-10	77.9	15.0	6.0	1.8	X
M-146	73.7	13.0	6.0	2.3	X
H-339	65.5	20.4	11.1	3.0	X
H-309	68.5	24.7	4.2	2.6	X
J-182	69.0	24.1	2.2	4.7	X
Average	70.8	20.4	5.9	2.9	X

X = presence noted

Location of above specimens

L.S.-10 and M-146: outcrop, center portion of dyke, south-east of main body

H-339 and H-304: drill-core, hole 1, 339 and 304 footage

J-182: drill-core, hole 2, 182 footage.

Field evidence indicates that the grey biotite-quartz-feldspar porphyry is intrusive. The evidence is in the form of a dyke of this material cutting sedimentary

rocks which was intersected in drill-holes 1 and 3, and by the intrusive contact displayed in the core from drill-hole 2. The relationship of grey biotite-quartz-feldspar porphyry to white quartz-feldspar porphyry however, has been obscured by intense quartz veining in their contact areas. A discussion of the relations between these two rock units is included in the section postulating the environment and history of the complex.

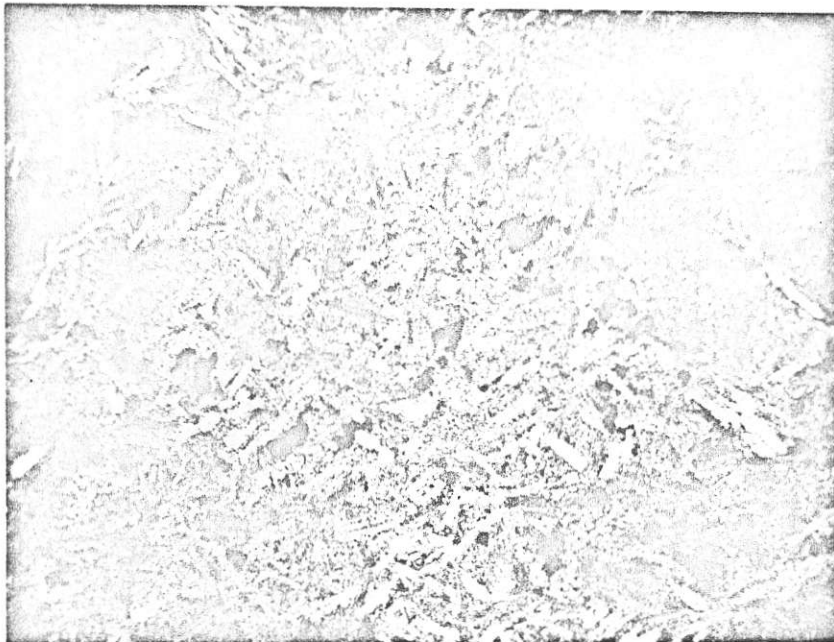
(iii) Dark Green Aphanitic Dykes

Dykes of this rock unit were observed only in core from drill-holes 1, 2, and 3 cutting grey biotite-quartz-feldspar porphyry and argillite-greywacke (see fig. 6). Core length intersections vary from 6 inches to 19 feet. The single dyke intersected in drill-hole 1 also occurs in hole 3. Its strike was determined to be N 38°E, because of the fact that the elevation of the intersections in both holes are the same. The attitudes of the other dykes are unknown.

The dykes are aphanitic, dark green in color, and contain fine-grained, disseminated pyrite. They are cut by carbonate shears and quartz-calcite veinlets containing pyrite and sparse molybdenite.

In thin-section (see Plate 4), the rock appears as a fine-grained (0.1 to 1 mm) aggregate of biotite and plagioclase. Biotite (50%) occurs as dark brown pleochroic clots





X 28, crossed nicols

Photomicrograph of dark green aphanitic dyke rock showing plagioclase (white laths), biotite (grey), and pyrite (black). Taken from drill-core, hole 1, footage 14.

Plate 4 - Dark green aphanitic dyke rock.

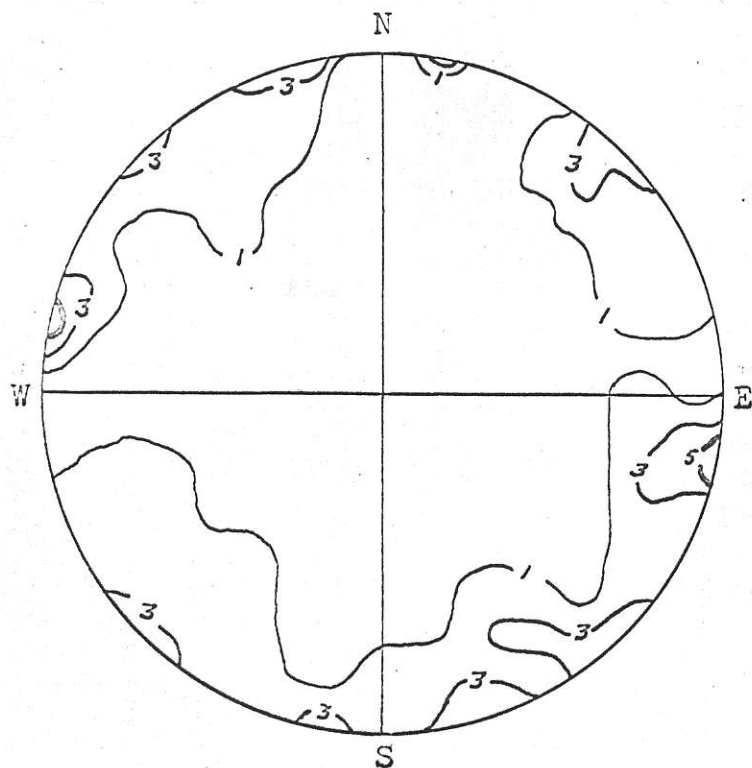
and disseminated flakes. Plagioclase (40%) forms tabular, albite-twinned crystals, whose composition is estimated as  $An_{10-20}$  (relative index of refraction slightly less than 1.54; average of maximum angles  $x' \wedge a = 5^\circ$ ). Pyrite (10%) appears to be the only accessory mineral and occurs as scattered, anhedral grains averaging 0.5 mm in diameter. The high biotite content of this rock type suggests it is a lamprophyre.

(iv) White Quartz-Feldspar Porphyry

As shown in fig. 4, white quartz feldspar porphyry, the most abundant of the igneous rock types, forms a highly irregular shaped body, approximately 3400 feet long in a northwesterly direction and 1000 to 1600 feet wide. A strong system of northeast striking and steeply dipping dykes project from the main body to the northeast and southwest. The north part surround what is believed to be a roof pendant of sedimentary rocks.

Very little is known of the subsurface shape of this rock type. On surface, contact inclinations are obscure because of the general lack of outcrop and the lack of distinct planar contacts with the sedimentary host rocks. Drilling information indicates that the southern contact is steeply dipping (see fig. 6).

Fracturing is most intense in the southeast portion, particularly in the proximity of the grey biotite-quartz-feldspar porphyry and the contact with the sedimentary rocks. It decreases towards the central and northern portions where recognizable joint planes spaced 6 inches to 2 feet apart can be measured. Their attitudes however, do not indicate any outstanding set (see fig. 8). At best it can only be said that jointing appears to be highly irregular in strike and predominantly steep in dip, with a 5 pole maximum in fig. 8 suggestive of a predominant (weak) northeast strike and near vertical dip. The northern portion shows a well developed shear direction, trending north to northwest and variable in the direction of dip.



- 57 poles plotted from field observations.
- lower hemisphere equal area projection.
- contour interval 1, 3, and 5 poles.

Fig. 8 - Contour diagram of poles to joints in white quartz-feldspar porphyry.

The white quartz-feldspar porphyry varies in the degree of alteration, the size and number of phenocrysts, the biotite content, the pyrite content, and the presence of inclusions. The inclusions are of sufficient number in some places to make the rock appear as a breccia. The distribution of pyrite and inclusions is shown in fig. 4.

For the most part, the rock is a brilliant white color, and contains one to three mm phenocrysts of quartz and feldspar set in an aphanitic matrix. Biotite and chlorite are rare, with a patchy distribution, but are most frequently observed in the central part of the porphyry in the vicinity of specimens M-60 and L.S.-41 (see fig. 7). In drill-core, it appears in the lower intersections of the white porphyry in drill-holes 1, 2, and 3.

Disseminated pyrite appears in the white quartz-feldspar porphyry in the north-central portion, and in the southern portion northeast and southwest of the grey biotite-quartz-feldspar porphyry. In the highly pyritic areas depicted in fig. 4, the pyrite content is estimated to be 1 to 5 volume per cent.

North of the northern highly pyritic area, dendritic coating of manganese dioxide (pyrolusite) are frequently observed on outcrop surfaces and joint planes. East of the pond, the porphyry is light grey and contains small (2 to 3 mm) clots of light green epidote (L.S.-56). To the west of

the pond (L.S.-57), the porphyry is a brilliant white and contains visible feldspar phenocrysts. Pyrite also occurs in this northern part but does not approach the concentration of that in the highly pyritic areas.

Very fine-grained porphyry, in which 0.5 to 1 mm diameter phenocrysts of quartz can be recognized, occurs in the contact area of the southern part of the complex. This variation is typical of specimens from the dyke areas northeast and southwest of the grey biotite-quartz-feldspar porphyry and core from drill-hole 4.

The inclusions, which range from one-tenth to one inch in diameter, are found in the highly pyritic white quartz-feldspar porphyry in the north and throughout the contact portions of white quartz-feldspar porphyry in the south part of the complex. Drill-hole 4 is reported to contain abundant inclusions within the porphyry intersection. Most of the inclusions can be visibly recognized as sedimentary rock fragments. In the northern pyritic area, quartz-veined, quartz-feldspar porphyry fragments occur within the white quartz-feldspar porphyry in the outcrops of specimens L.S.-50, -54, and -59. In outcrops of L.S.-50 and -59, the quartz veinlets in the fragments contain molybdenite. Similar occurrences are reported from drill-hole 4.

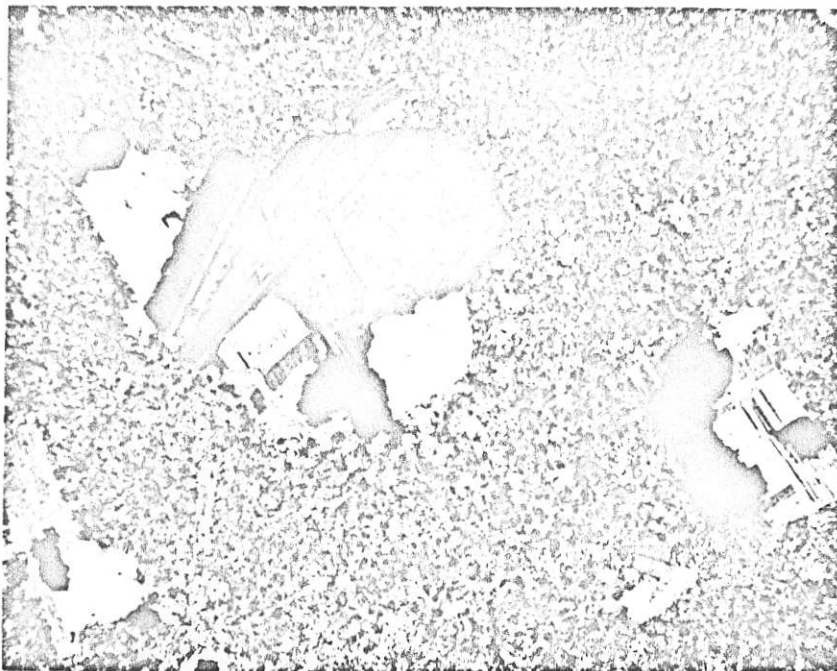
In the microscopic examination of thin-sections of white quartz-feldspar porphyry, it was found that all contain at least some signs of alteration. The most common alteration mineral was fine-grained, white mica of high birefringence, hereafter called "sericite". The thin-sections showing the least alteration are L.S.-42, -43, -47, -48, -49, and -57. Modal analyses (point count method) of these are given in Table II. The rocks in these thin-sections are similar; they contain 0.5 to 3.0 mm euhedral to subhedral phenocrysts of quartz, unzoned plagioclase (see Plate 5), potash feldspar that appears to be optically homogenous, and very minor amounts of medium to light brown biotite partially altered to chlorite. The matrix is very fine-grained (0.05 mm) potash feldspar and quartz. Minor amounts of sericite occur as scattered flakes throughout the matrix and in plagioclase phenocrysts. Apatite and zircon (0.1 mm) are present in very minor quantities.

Table II

Modal Analyses of White Quartz-Feldspar Porphyry

Thin-section Number	Volume %						
	Matrix	Albite	Potash Feldspar	Quartz	Biotite	Pyrite	Sericite
L.S.-57	82.5	7.57	4.75	5.93	X	X	X
L.S.-42	85.0	7.31	1.61	5.61	X	X	X
L.S.-48	83.0	7.70	.70	8.22	.35	X	X
L.S.-47	84.2	7.45	1.30	6.90	.15	X	X
L.S.-43	81.7	7.50	2.20	8.20	.40	X	X
L.S.-49	84.9	7.60	3.00	5.50	X	X	X
Average	83.50	7.52	2.26	6.72	.15	X	X

X = presence noted



X 20, crossed nicols

Photomicrograph of unzoned albite phenocrysts  
in white quartz-feldspar porphyry. Taken from  
thin-section L.S.-49, outcrop.

Plate 5 - White quartz-feldspar porphyry.

The phenocrysts of quartz, unzoned plagioclase, and optically homogeneous potash feldspar are interpreted as primary minerals produced during the crystallization of the porphyry magma. This origin is indicated by their euhedral outline and porphyritic texture. Potash feldspar phenocrysts appear to be later in terms of the crystallization sequence of the phenocrysts as they are commonly observed partially surrounding quartz and plagioclase.

Unzoned plagioclase and optically homogeneous potash feldspars are generally found in all the thin-sections examined. Plagioclase in some cases has been obliterated by alteration. Universal stage techniques, using the Fedorow method outlined in Emmons (1943) were used to determine their optical properties with respect to their crystallographic elements. The results of this work follows.

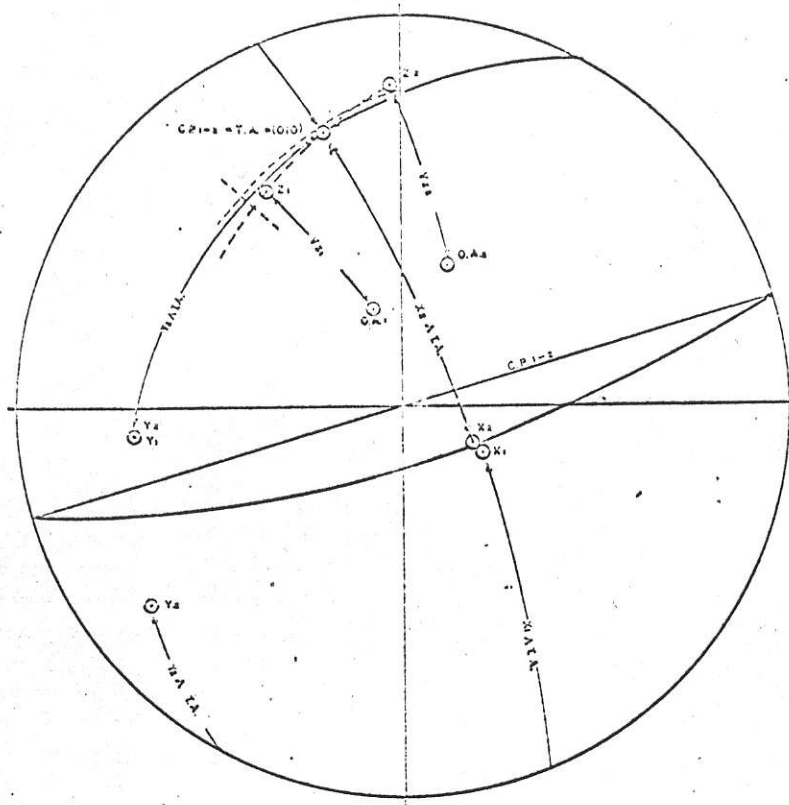
(a) Plagioclase feldspar

The composition and the structural state of the plagioclase feldspars was derived through application of the optical properties to graphs given in Slemmons (1962). In brief, Slemmons method consists of measuring optic orientations in two adjacent individuals in a twinned plagioclase, the composition plane, and any crystallographic directions such as cleavages, or crystal faces. These are plotted on a lower hemisphere stereographic projection from which ang-



ular measurement can be derived and applied to migration curves to determine the composition and the structural state of the plagioclase feldspar. The migration curves for feldspars formed under plutonic conditions differ from those formed under volcanic conditions. Thus, depending upon which curve the plagioclase feldspar plots follow, an interpretation of the crystallization conditions can be derived. If the angles derived fall between the two curves, Slemmons thinks that hypabyssal conditions likely prevailed. An example universal stage determination of the angles considered in this method, using an albite-twinned plagioclase phenocryst, is illustrated in fig. 9 .

In this study, 5 separate plagioclase phenocrysts were studied in the above manner. In each, adjacent twins of the albite twin law were used. In all 5, the feldspar is optically unzoned and the refractive index is slightly less than that of Canada balsam ( $n_{rel.} < 1.54$ ). The refractive index alone suggests the composition to be  $Ab_{75}An_{25}$ . In all 5, the derived angles are similar (see Table III).



1,2 = two adjacent albite twin lamellae  
C.P.= composition plane  
T.A.= twin axis  
O.A.= optic axis  
X,Y,Z= optic directions  
- example from thin-section L.S.-21  
plotted on lower hemisphere stereographic  
projection.

Fig. 9 - Universal stage orientation and derivation of XATA and YATA for two adjacent albite twin lamellae in plagioclase.

Table III

2V, X $\wedge$ TA, and Y $\wedge$ TA of Albite-twinned  
Plagioclase in White Quartz-Feldspar Porphyry

Thin-section	2V <sub>Z</sub>	Y $\wedge$ TA	X $\wedge$ TA
M-5	79°	74°	89.5°
L.S.-14	79°	74°	89°
L.S.-21	77°	74°	88°
L.S.-49	78°	74°	89.5°
L.S.-57	81°	74°	88°

The application of the angles for X $\wedge$ TA and Y $\wedge$ TA to the migration curves for the albite twin law (see fig. 10) indicates one of two plagioclase compositions derived under plutonic conditions: Ab<sub>98</sub>An<sub>2</sub> or Ab<sub>32</sub>An<sub>68</sub>. However, the 2V<sub>Z</sub> values are positive, and range from 77° to 81°. Therefore, the composition is derived as being Ab<sub>98-95</sub>An<sub>2-5</sub> (see fig. 11).

Thus, the unzoned plagioclases of the white quartz-feldspar porphyry are albite in composition and crystallized under plutonic conditions.

(b) Potash Feldspar

The 2V values and extinction angles on (010) (X'  $\wedge$  (001) cleavage) were obtained from optically homogeneous potash feldspar phenocrysts in 4 separate thin-sections. The results are listed in Table IV. All except specimen L.-534 (baveno-twinned) are measurements of Manebach-twinned crystals.

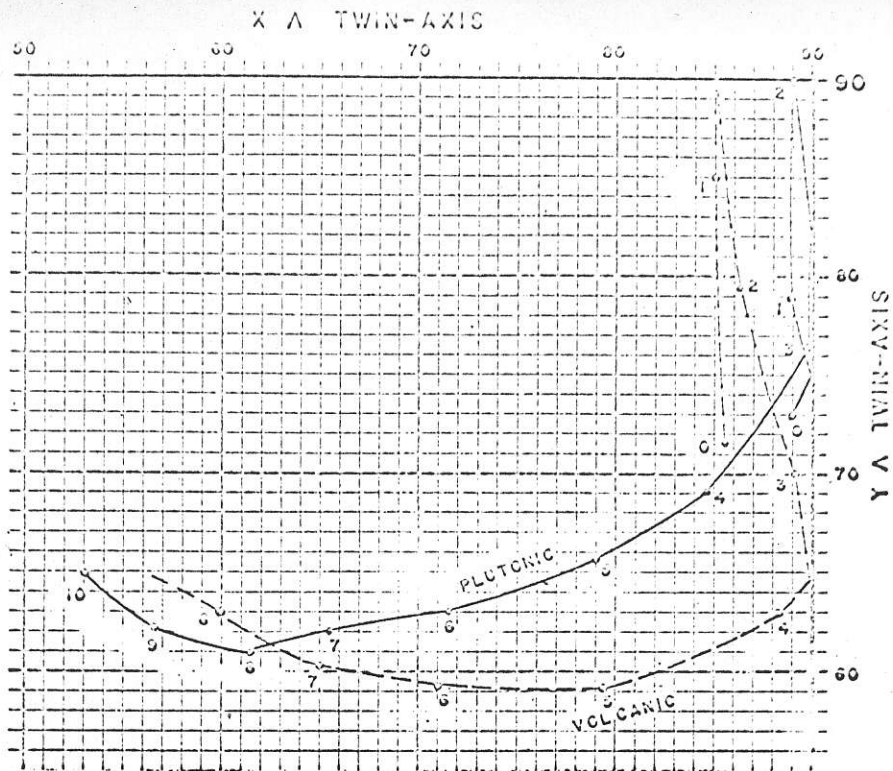


Fig. 10 - Twinning-axis Curves for the Albite Twin Law.  
(after Slemmons, 1962)

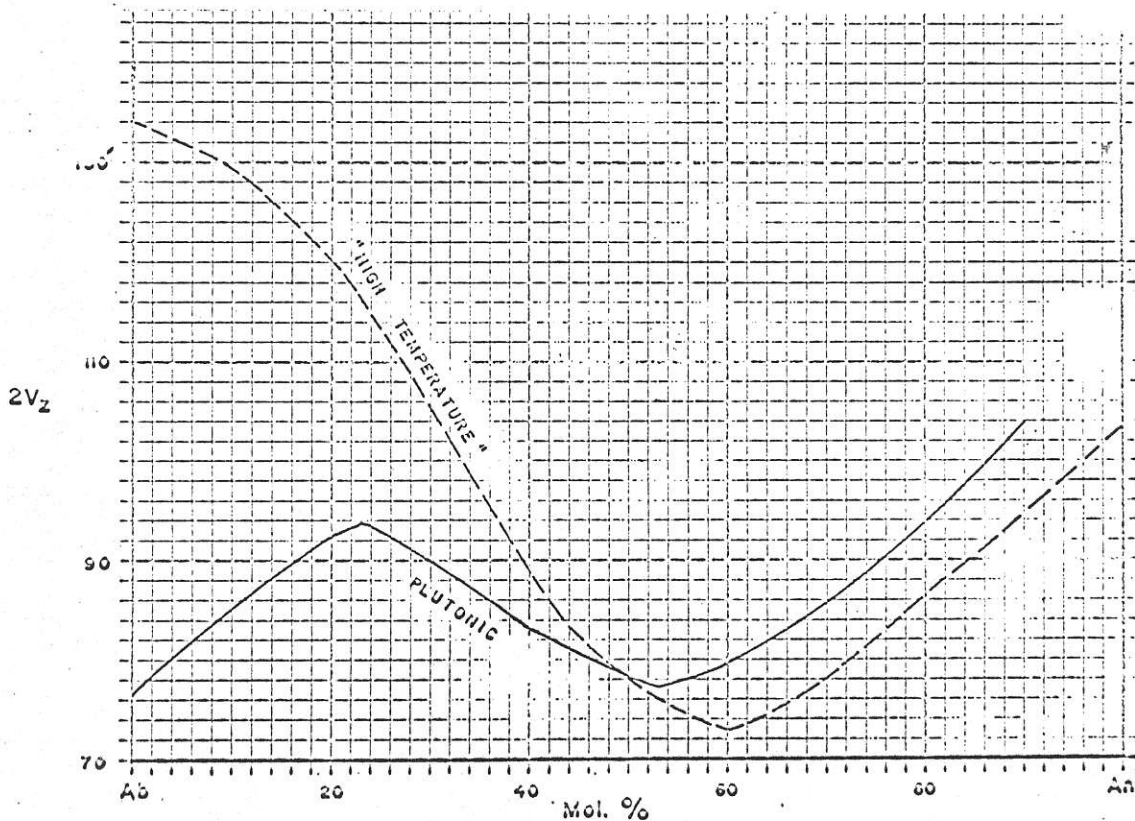


Fig. 11 -  $2V_z$  Values for Plutonic and "High Temperature"  
Plagioclases. (after Slemmons, 1962)

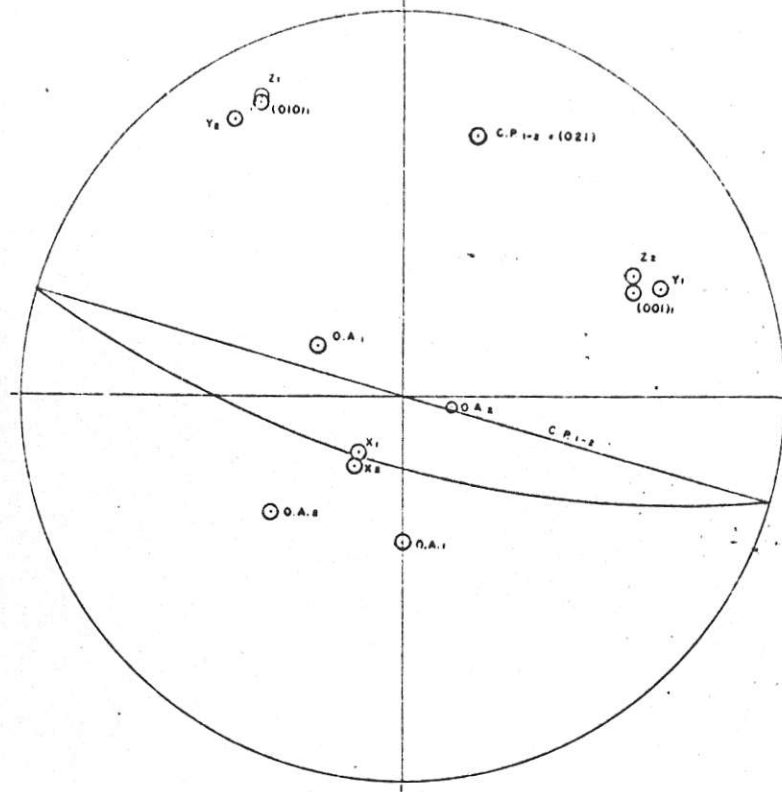
Table IV

2V Values and Extinction Angles on  
(010) for Potash Feldspar Phenocrysts.

Thin-section	Location	(-)2V	Extinction on (010)
L.S.-43	see fig. 7	53°	5°
L.S.-57	"	53°	5°
L.S.-38	"	56°	6°
L.-534-B	drill-hole 4, 534 foot- age	61°	4°

The Baveno-twinned crystal of L-534-B is shown in stereographic projection in fig. 12. The fact that the pole to (010) coincides closely with Z is important as it shows that the potash feldspar is orthoclase. In microcline, Z makes an angle of 18° with the perpendicular to 010; in anorthoclase, the angle is 5° (Deer, Howie and Zussman, 1963). The writer therefore interprets the optically homogeneous potash feldspar phenocrysts as being orthoclase, having a (-)2V ranging from 56° to 61° and an extinction on (010) of 4° to 6°. This derivation is supported by the evident lack of combined albite and pericline twinning, which is characteristic of microcline.

In summation, the basic character of white, quartz-feldspar porphyry resulting from the primary crystallization of the responsible magma is: 0.5 to 3 mm phenocrysts of quartz, unzoned plagioclase ( $Ab_{92-98} An_{8-2}$ ), optically homogeneous



- 1, 2 = two adjacent baveno twin lamellae.
- C.P. = composition plane.
- O.A. = optic axis.
- Y, Y, Z = optic directions.
- example from thin-section from drill-hole 4, footage 534, plotted on lower hemisphere stereographic projection.

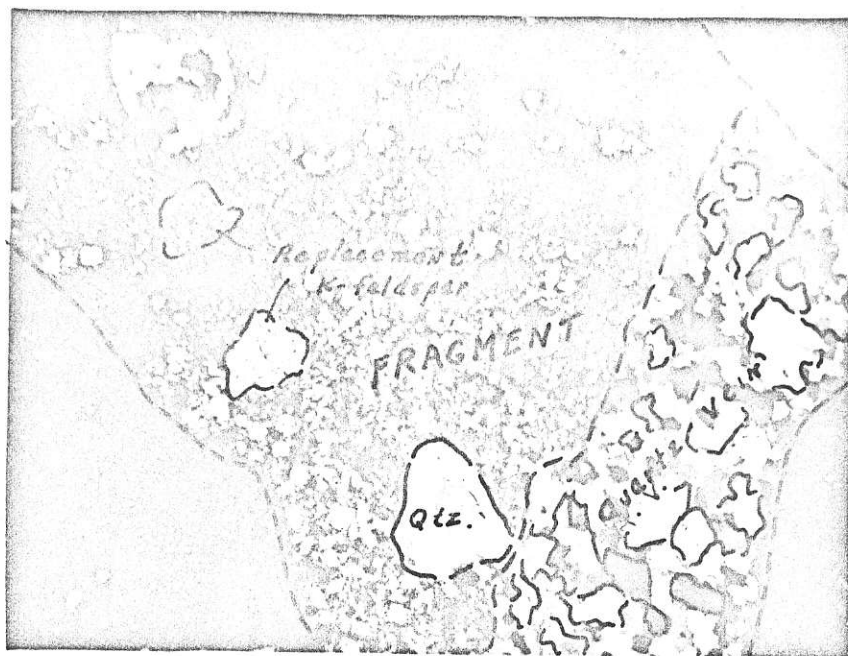
Fig. 12 - Universal Stage Orientation of Baveno Twin, Potash Feldspar Phenocryst.

orthoclase, and erratically distributed pale brown biotite, all set in a very fine-grained matrix of potash feldspar, sericite, and quartz.

Under the microscope, thin-sections of the fine-grained porphyry (L.S.-20, -21, -22), have minerals similar to those present in the average white quartz-feldspar porphyry (thin-sections of Table II). The phenocrysts total about 5 per cent of the volume of the rock and tend to blend in with the matrix, thus giving a porcelaneous texture to the rock.

Thin-section studies indicate that most, but not all, of the inclusions are fragments of sedimentary country rock. A few fragments of quartz-veined, quartz-feldspar porphyry (see Plate 6), similar to the white quartz-feldspar porphyry host, are present. The thin-sections containing this type of fragment are from the north part of the complex (L.S.-50, -54, -59) and a number of thin-sections of core from drill-hole 4. In both localities, the quartz veinlets in the fragments contain minor amounts of molybdenite. In drill-hole 4, the fragments and the rock surrounding them are in turn cut by quartz-molybdenite veinlets, indicating two periods of mineralization.

One inclusion observed in a thin-section (see plate 7)

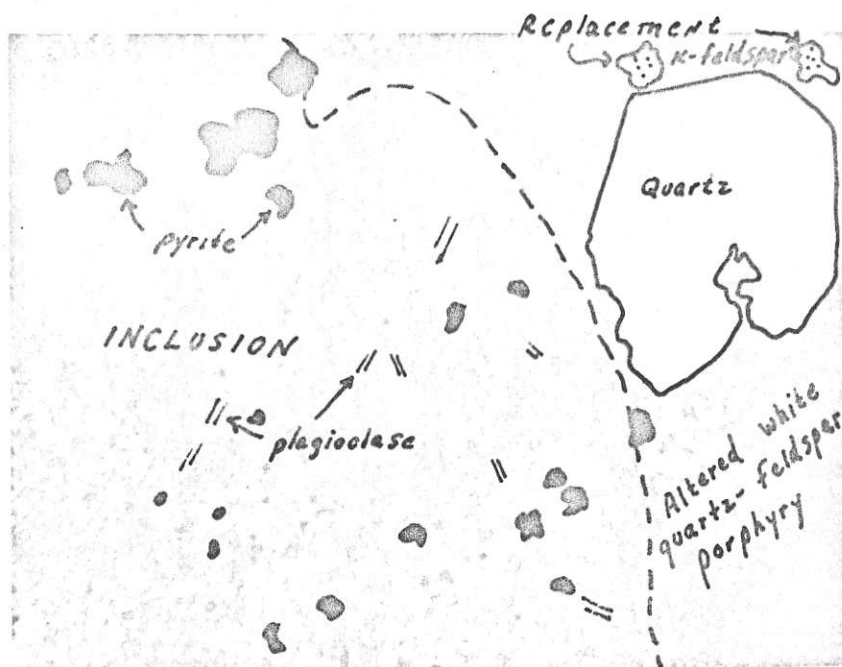


X 27, crossed nicols

Photomicrograph shows a quartz-veined fragment of white quartz-feldspar porphyry surrounded by very fine-grained white quartz-feldspar porphyry. The fragment (outlined by the dotted orange line) occupies the center of the photograph. The quartz vein occurs on the right side of the fragment.

Plate 6 - Quartz-veined fragment of white quartz-feldspar porphyry included in a groundmass of very fine-grained white quartz-feldspar porphyry.





X 30, crossed nicols

Photomicrograph of possible inclusions (middle and left side of photo) of dark green aphanitic dyke rock in white quartz-feldspar porphyry (right side of photo). Plagioclase occurs as white laths, chlorite (after biotite?) as dark grey grains, pyrite as black grains. The texture and mineralogy bears a very close resemblance to the dyke unit (compare with plate 4). Taken from drill-core, hole 4, footage 652.

Plate 7 - Possible inclusion of dark green aphanitic dyke rock in breccia portion of white quartz-feldspar porphyry.

from drill-hole 4, footage 652, resembles the dark green aphanitic dyke rock in that it contains similar albite-twinning plagioclases, abundant chlorite (after biotite?) and fine-grained pyrite. This observation implies that the dark green aphanitic dykes were emplaced prior to the white quartz-feldspar porphyry.

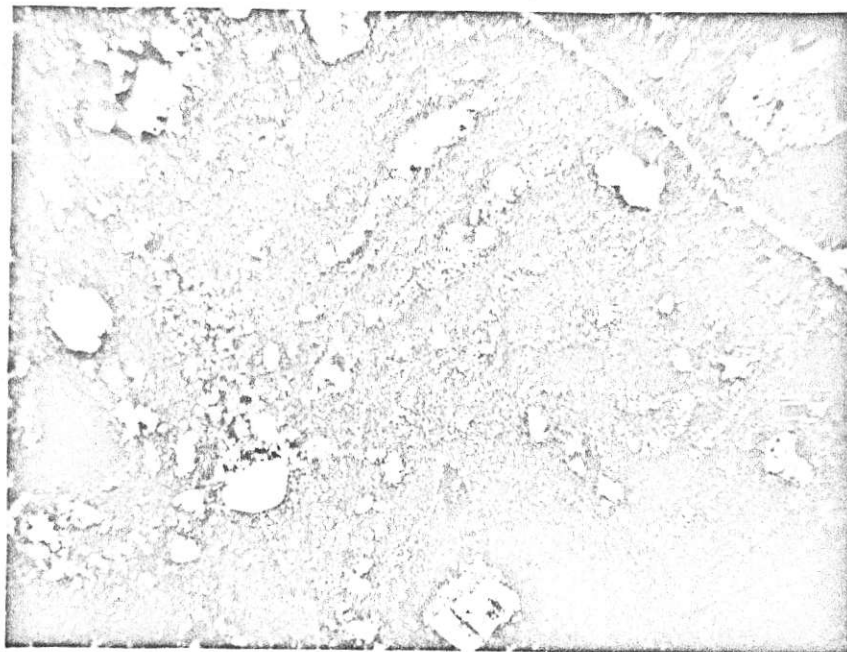
Thin-sections from core in drill-hole 4 where there is a high number of inclusions (approximately 20 to 40 per cent by volume), show cataclastic features in which the phenocrysts have been broken into angular fragments (see plate 8).

Portions of the white quartz-feldspar porphyry are intensely altered. The alteration types recognized are: intense sericitization, feldspathization, epidote-calcite replacement of plagioclase, the development of clay minerals in intensely quartz-veined areas, and pyritization. A more detailed description is included in the section on alteration.

(v) Alaskite Dykes

Surface exposures of this rock type occur as northwest to northeast trending dykes, 1 to 4 feet thick, cutting the argillite-greywacke sequence on the southeast edge of the complex. Similar dykes were seen in core from drill-holes 1, 3, and 4, all within sedimentary rock.

The alaskite is light green to cream in color with



X 27, crossed nicols

Photomicrograph of white quartz-feldspar porphyry showing granulation and flow structures. Taken from thin-section of drill-core, hole 4, footage 652.

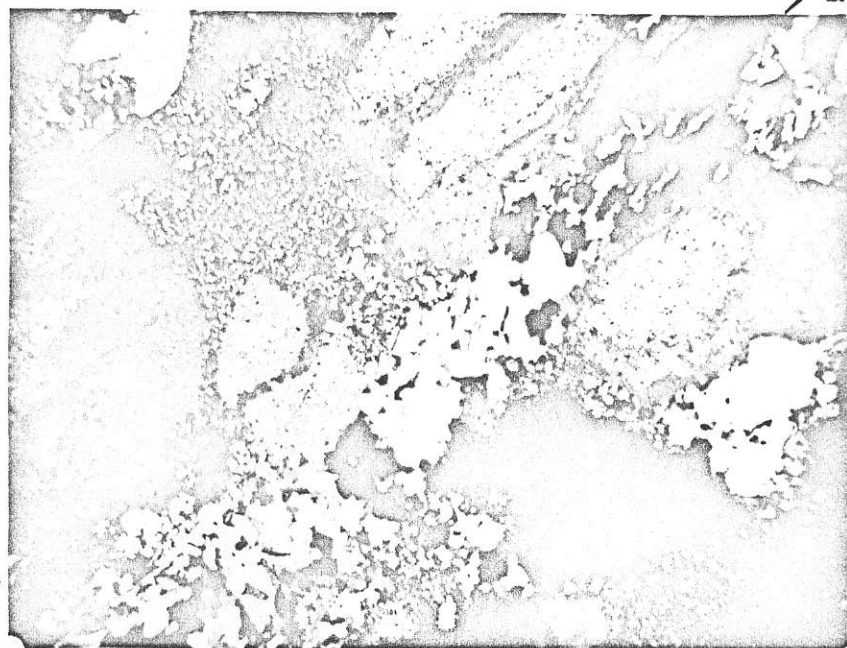
Plate 8 - Cataclastic structure in white quartz-feldspar porphyry.

a granitic appearance in hand specimen. The feldspar and quartz grains average 2 to 4 mm in diameter. The dykes are highly fractured and cut by narrow quartz veinlets, both barren and mineralized with pyrite and fine-grained molybdenite.

Thin-sections show that this rock actually has a porphyritic texture (see plate 9). The phenocrysts present are quartz and unzoned plagioclase feldspar that has been extensively replaced by potash feldspar and to a lesser extent by sericite. The matrix is a very fine-grained (0.1 mm and less) aggregate of quartz, potash feldspar, and minor sericite. The phenocrysts are estimated as being 80% of the volume of the rock.

The very ragged outline of the potash feldspar-rimmed plagioclase crystals makes it difficult to determine if this is a true porphyry. It is possible that the porphyritic texture may be a result of either protoclasis or cataclasis.

A single measurement of an albite-twinning plagioclase phenocryst by universal stage methods gave  $(+)2V=78^\circ$ ,  $X\lambda TA=90^\circ$ ,  $Y\lambda TA=73^\circ$ . According to Slemmons graphs (figures 10, 11), the composition is in the vicinity of  $Ab_{98}An_2$ . The similarity to the plagioclase composition in the white quartz-feldspar porphyry suggests the two rock types are related.



Quartz  
veinlet.

X 20, crossed nicols

Photomicrograph of the alaskite showing extensive replacement of plagioclase (white) by potash feldspar (grey). Quartz-molybdenite veinlet cuts section from top right corner to lower left corner. Taken from thin-section L.S.-31, outcrop.

Plate 9- Alaskite dyke unit.

Chemical Analyses and Classification of the Igneous  
Rock Units of the Complex

Chemical analyses of the igneous rock units of the complex are given in Table V. In the case of the alaskite dyke rock unit, only  $K_2O$ ,  $CaO$ , and  $Na_2O$  analyses are given. Comparative analyses from Nockolds (1954) are given in Table VI. The locations of the analysed samples are shown in fig. 7. Thin-sections were cut from all specimens which were chemically analyzed. On the basis of these studies, the following conclusions may be stated.

(i) Pink quartz porphyry

The pink quartz porphyry (analysis 1 in Table V) is relatively rich in  $K_2O$  and poor in  $Na_2O$  and  $CaO$ . No minerals or textural features indicating potash metasomatism processes were observed in thin-sections of this rock type. Therefore, the analysis is interpreted as giving the primary composition of this rock unit. No comparative analyses having as high  $K_2O$  and low  $Na_2O$  and  $CaO$  content are listed by Nockolds (1954). The closest comparative analyses is alkalic granite. Thus, a suitable classification term for pink quartz porphyry is a very high potash granite.

(ii) Grey biotite-quartz-feldspar porphyry

The two analyses of grey biotite-quartz-feldspar porphyry correspond closely to those of muscovite-biotite-adamellite listed in Nockolds' tables. Adamellite is more

Table V

Chemical Analyses of Igneous Rock Types

Analysis No. (Thin-section)	SiO <sub>2</sub>	TiO <sub>2</sub>	Al <sub>2</sub> O <sub>3</sub>	Fe <sub>2</sub> O <sub>3</sub>	MnO	CaO	Na <sub>2</sub> O	K <sub>2</sub> O	MgO	H <sub>2</sub> O	P <sub>2</sub> O <sub>5</sub>	CO <sub>2</sub>	Total
1. (L.S.-53)	74.60	n.d.	13.00	1.24	n.d.	0.14	0.16	10.20	n.d.	0.59	0.06	n.d.	99.99
2. (H-339)	73.50	0.24	14.20	1.60	n.d.	1.48	2.16	4.92	1.20	1.04	0.06	n.d.	100.40
3. (M-146)	74.80	0.20	14.50	0.60	n.d.	1.20	2.77	4.08	1.45	0.62	0.08	n.d.	100.30
4. (H-14)	48.35	1.19	18.60	9.70	0.22	2.65	2.51	7.29	6.72	1.27	0.43	0.08	99.06
5. (L.S.-57)	74.20	0.10	13.65	1.00	0.05	0.20	2.05	6.45	1.06	0.88	0.11	n.d.	99.75
6. (L.S.-47)	74.40	0.10	14.05	0.95	n.d.	0.25	2.42	5.02	1.00	0.65	0.07	n.d.	98.91
7. (L.S.-49)	74.40	0.09	14.00	1.16	n.d.	0.36	1.75	5.40	1.00	0.48	0.10	n.d.	98.74
8. (H-1165)	73.70	0.10	13.65	1.40	n.d.	1.25	2.65	4.80	1.30	0.77	0.10	0.74	100.46
9. (M-5)	76.00	0.06	13.65	n.d.	n.d.	0.12	2.45	5.60	0.95	0.55	0.08	n.d.	99.46
10. (L.S.-38)	76.65	0.02	11.80	0.02	n.d.	Tr.	0.50	8.22	0.60	0.47	0.07	n.d.	98.35
11. (T-14)	74.00	0.01	13.20	n.d.	n.d.	n.d.	0.56	9.83	0.85	0.55	0.11	n.d.	99.11
12. (L.S.-31)	-----Partial analysis-----					0.30	3.08	5.38	-----				
13. (L.S.-31)	-----Partial analysis-----					0.35	4.70	5.88	-----				

n.d. = not detected  
 Tr. = trace  
 Fe<sub>2</sub>O<sub>3</sub> = total iron as Fe<sub>2</sub>O<sub>3</sub>  
 - Na<sub>2</sub>O by flame photometer  
 - P<sub>2</sub>O<sub>5</sub> by colorimetric method  
 - CO<sub>2</sub> by acid treatment  
 - remaining oxides by X-ray fluorescence, K. Ramlal, analyst, University of Manitoba.

Analysis No.

Rock Types

1. = pink quartz porphyry, from outcrop.
2. = grey biotite-quartz porphyry, from drill-hole 1, footage 339
3. = grey biotite-quartz-feldspar porphyry, from dyke, south end of complex.
4. = dark green aphanitic dyke, from drill-hole 1, footage 14.
- 5,6,7, = least altered white quartz-feldspar porphyry, from outcrops.
8. = altered white quartz-feldspar porphyry, cut by quartz-calcite veinlets, contains approximately 1.5% biotite/chlorite. From drill-hole 1, footage 1165.
9. = altered white quartz-feldspar porphyry, moderate replacement potash feldspar, from outcrop.
- 10,11. = altered white quartz-feldspar porphyry, intense replacement potash feldspar, from outcrop.
- 12,13. = alaskite dykes, from outcrop.

Table VI

Comparative Analyses From Nockolds (1954)

	Muscovite-biotite Adamellite	Average Alkali Granite *
SiO <sub>2</sub>	71.86	73.86
TiO <sub>2</sub>	00.30	0.20
Al <sub>2</sub> O <sub>3</sub>	14.73	13.75
Fe <sub>2</sub> O <sub>3</sub>	0.64	0.78
FeO	1.61	1.13
MnO	0.04	0.05
MgO	0.67	0.26
CaO	1.51	0.72
Na <sub>2</sub> O	3.18	3.51
K <sub>2</sub> O	4.64	5.13
H <sub>2</sub> O	0.66	0.47
P <sub>2</sub> O <sub>5</sub>	0.16	0.14

commonly known as quartz monzonite.

(iii) Dark green, aphanitic dykes

The analysis of the dark green, aphanitic dyke unit is characterized by high  $K_2O$ ,  $Na_2O$ ,  $MgO$ , and  $Fe_2O_3$  content. According to Turner and Verhoogen (1951) rocks having this chemical aspect are in general typical of lamprophyres:

"Chemically the lamprophyres are basic to ultrabasic rocks with a high content of both  $(FeO + MgO)$  and  $(Na_2O + K_2O)$ , expressed mineralogically by abundance of biotite and barkevikitic hornblende."

(iv) White quartz-feldspar porphyry

Six analyses of white quartz-feldspar porphyry were completed. The thin-sections of the rocks corresponding to analyses 5, 6, and 7 contain only scant sericite as a definite alteration mineral. A thin-section of the rock corresponding to analysis 9 shows scant amounts of potash feldspar as a replacement of the plagioclase phenocrysts, but this analysis is not markedly different from analyses 5, 6, and 7. Therefore, analyses 5, 6, 7, and 9 are considered to be closely representative of the primary composition of this rock type. The analyses of samples 5, 6, 7, and 9 are in close correspondence to the average alkali granite listed in Nockold's tables but have somewhat lower  $CaO$  and  $Na_2O$  contents.

Analysis 8 is white quartz-feldspar porphyry which is cut by quartz veinlets and contains approximately 1.5 per cent biotite. In thin-section, it was found that the calcite



is associated with the quartz veins, thus accounting for the relatively high CaO content. A correction for calcite using the 0.74 per cent CO<sub>2</sub> present in the analysis suggests the original CaO content may be in the order of 0.3 per cent.

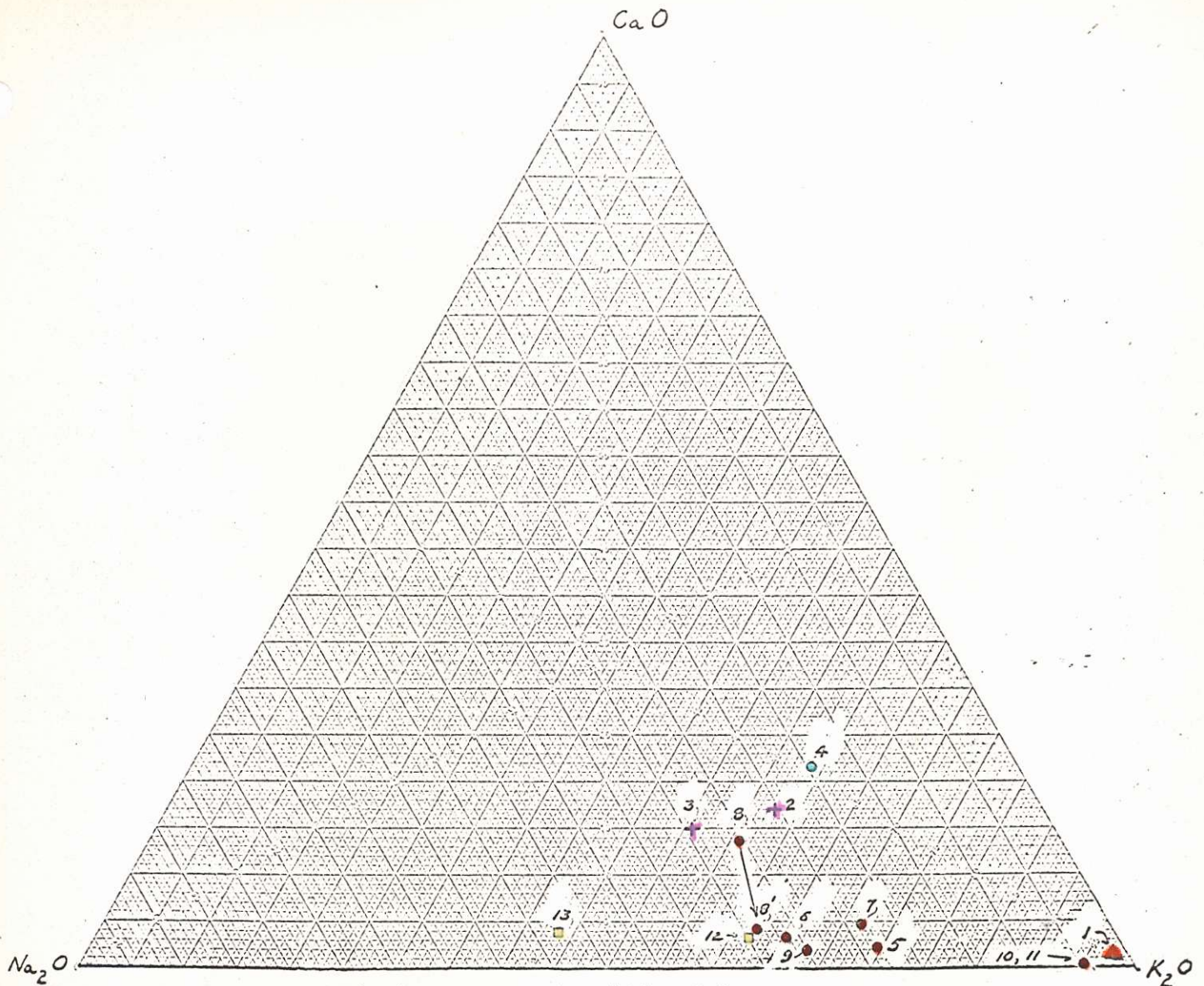
The thin-sections of rocks corresponding to analyses 10 and 11 show that the plagioclase phenocrysts have been replaced almost entirely by potash feldspar. In comparison with analyses 5, 6, 7 and 9, the analyses of 10 and 11 are relatively richer in K<sub>2</sub>O and poorer in Na<sub>2</sub>O and CaO. It is believed that the increase in K<sub>2</sub>O is due to hydrothermal alteration processes.

(v) Alaskite dykes

Only partial analyses of this rock type have been obtained (analyses 12, 13). However, the K<sub>2</sub>O, Na<sub>2</sub>O and CaO content of this rock unit classifies it as an alkali granite. The analyses may not be truly representative of the primary composition as corresponding thin-sections show extensive replacement of plagioclase by potash feldspar. The replacement processes are believed to be hydrothermal in view of the highly quartz-veined aspect of this rock.

A triangular diagram of the weight percentages of K<sub>2</sub>O, Na<sub>2</sub>O, and CaO of the analyses of the igneous rock units of the complex is shown in fig. 13. C.I.P.W. normative minerals are listed in Table VII.

In summation, chemical analyses classify the five



- = dark green aphanitic dyke
- ✦ = grey biotite-quartz feldspar porphyry
- = white quartz-feldspar porphyry
- = alaskite dykes
- ▲ = pink quartz porphyry

Note: numbers correspond to analyses in Table V.  
The plot of 8' corresponds to analysis 8  
after correcting for CaO and CO<sub>2</sub> in calcite.

Fig. 13 - Triangular diagram of the weight % of K<sub>2</sub>O, Na<sub>2</sub>O,  
and CaO from analyses of Table V.

Table VII

C.I.P.W. Normative Minerals of the Four Porphyry Rock Units

Analysis Number	Norm in Weight %						
	Quartz	Orthoclase	Albite	Anorthite	Apatite	Calcite	Corundum
1.	84.85	80.00	1.85	.57	.03	--	1.45
2.	88.02	29.03	13.23	7.22	.03	--	2.68
3.	40.58	24.12	28.42	5.78	.11	--	2.98
5.	87.28	88.14	17.29	.77	.15	--	2.99
6.	40.67	29.68	20.48	1.03	.09	--	4.28
7.	42.90	81.91	14.77	1.58	.14	--	4.68
8.	88.40	28.70	22.71	1.22	.14	1.68	3.64
9.	40.15	88.07	20.89	.54	.11	--	3.42
10.	45.20	47.80	4.00	--	--	--	2.11
11.	88.18	58.11	4.71	--	--	--	1.62
12.	--	80.98	25.45	1.47	--	--	--
13.	--	84.76	39.67	1.72	--	--	--

note:

Normative minerals are calculated according to C.I.P.W. rules, with the exception that instead of allotting one-half of CaO to form wollastonite, all CaO is used to form anorthite after allowing for calcite and apatite. This is in keeping with the observed mineralogy of the rock units. Ilmenite, magnetite, hematite, enstatite, and ferrosilite have been deleted from the norm calculations.

rock units of the complex as:

- (i) Very potash-rich granite = pink quartz porphyry.
- (ii) Biotite-muscovite adamellite (or quartz monzonite) = grey biotite-quartz-feldspar porphyry.
- (iii) Lamprophyre = dark green aphanitic dykes.
- (iv) Alkali granite = white quartz-feldspar porphyry.
- (v) Alkali granite = alaskite dykes.

The significance of the differences in mineralogy and chemical composition of the rock units with regard to the environment and history of the complex is discussed in the final chapter on interpretations and conclusions.

CHAPTER IV - MOLYBDENITE MINERALIZATION AND  
HYDROTHERMAL ALTERATION

Molybdenite Mineralization

All the observed molybdenite mineralization on the Lucky Ship property occurs as very fine-grained (0.5 mm and less) flakes in quartz veinlets. Sparse quantities of pyrite are associated with the molybdenite. Chalcopyrite was noted in drill-core, but only in trace amounts. Calcite occurs in varying quantities in both mineralized and barren quartz veinlets. The thickness of individual veinlets vary from "hair-line" to 6 inches and average one-quarter inch in thickness. Several periods of mineralized and barren quartz vein emplacement are indicated by cross-cutting relationships. The number and apparent randomness of the veinlets classifies the mineralization as a stockwork type of deposit.

The known distribution of molybdenite mineralization in outcrops and diamond drill-holes is shown in figures 4 and 6. Except for the pink quartz porphyry, mineralization has been found in every rock type of the igneous complex and the immediately surrounding sedimentary rocks. The greatest known intensity of both mineralized and non-mineralized quartz veinlets occurs in the southeastern part of the complex. The best molybdenite mineralization observed in outcrop occurs in the alaskite dykes south of the south tie-line/63

and in the white quartz-feldspar porphyry north of the base line/63.

The outcrops of grey biotite-quartz-feldspar porphyry have many quartz veins, but the molybdenite is scarce.

Scattered minor occurrences of molybdenite are present in outcrops in the central and northern part of the white quartz-feldspar porphyry. In these outcrops, the molybdenite occurs in quartz-veined angular fragments of white quartz-feldspar porphyry included in the white quartz-feldspar porphyry. Similar mineralization occurs in drill-hole 4.

Very scant molybdenite in minor quartz veinlets was observed in a single outcrop of white quartz-feldspar porphyry approximately 800 feet south-southeast of the pond.

The distribution of molybdenite mineralization encountered in diamond drilling is shown graphically by plotting the number of mineralized veinlets per 10 feet of core length (see fig. 6). Generally, the number of mineralized veinlets bears a direct relationship to the  $\text{MoS}_2$  assays. Drill core indicates that the best mineralization occurs in the white-quartz feldspar porphyry and alaskite dyke intersections. The grey biotite-quartz feldspar porphyry is relatively poor in  $\text{MoS}_2$  (assays of 0.05 and lower).

From a general view, based on observed mineralization in outcrop (see fig.4), it appears that molybdenite mineralization is arranged concentrically about the grey biotite-

quartz-feldspar porphyry. This suggests a genetic relationship of the mineralization to this rock type. The more detailed picture obtained from drill-core shows that the mineralization is more closely related to the marginal portions of the white quartz-feldspar porphyry. The upper intersection of drill-hole 2 contained very little mineralization; a result which may be explained by the absence of white quartz-feldspar porphyry. Therefore, the apparent concentric distribution of mineralization about the grey biotite-quartz-feldspar porphyry as derived from observed outcrop mineralization does not hold true, in terms of relative abundance of molybdenite, in the drill-core from hole 2.

Alaskite dykes contain relatively abundant mineralization. This is particularly evident in drill-hole one. The dyke intersected in the upper part of the hole contains up to 50 mineralized veinlets per 10 feet of core, whereas the immediately surrounding sediments contain less than 20 veinlets per 10 feet of core.

The distribution of barren quartz veining in the drill-holes is also shown in fig. 6. The drill-core indicates that the fracturing and veining is in zones. The marginal portions of the white quartz-feldspar porphyry and the grey biotite-quartz-feldspar porphyry contain the highest number of barren veins. Therefore, the generalized picture obtained from outcrops, that the entire body of grey biotite-quartz-

feldspar porphyry is uniformly cut by numerous barren quartz veins, is incorrect.

#### Hydrothermal Alteration

White quartz-feldspar porphyry, grey biotite-quartz-feldspar porphyry, and alaskite dykes are hydrothermally altered. In the dark green aphanitic dykes, the alteration appears to be mainly chloritic alteration of biotite in proximity with quartz-carbonate veinlets. In the pink quartz porphyry, it is difficult to determine if significant alteration has taken place because of its extremely fine-grained texture. The sedimentary rocks have been intensely sericitized where in contact with the white quartz-feldspar porphyry and the alaskite dykes.

In the white quartz-feldspar porphyry, grey biotite-quartz-feldspar porphyry, and alaskite rocks, the alteration minerals present are typical of hydrothermal alteration (Schwartz, 1955). The principal alteration types recognized are sericitization, potash feldspathization, argillization, and saussuritization. Intense pyritization appears to be restricted to the portions of the white quartz-feldspar porphyry containing inclusions and the sedimentary rocks in contact with the igneous rocks of the complex. A description of the alteration types, with reference to thin-sections from outcrops (fig. 7) and drill core follows.



(i) Sericitization

Sericite occurs as very fine-grained flakes disseminated throughout the matrix and the plagioclase phenocrysts of the porphyries, and as seamlets adjacent to fractures and quartz veinlets. Thin-section studies indicate the least sericitized rock is the central part of the white quartz-feldspar porphyry (thin-sections L.S.-41, -42, -47, and -48), and the central part of the grey biotite-quartz-feldspar porphyry intersected by drill-holes 1 and 2 (see fig. 6).

The greatest quantities of sericite observed occur in the inclusion-rich portions (see fig. 4) of the white quartz-feldspar porphyry, and in the drill-core of the porphyries cut by abundant barren and mineralized quartz veinlets (see fig. 6).

(ii) Potash Feldspathization

Potash feldspar which has developed as an alteration mineral is apparent only in thin-sections. Furthermore, its development appears to be restricted to white quartz-feldspar porphyry and the alaskite dykes in the southern part of the complex. All the thin-sections of these two rock types from south of the North Tie Line/63 (see fig. 7) show some potash feldspars developed as an alteration mineral.

In thin-sections, the potash feldspar appears in two forms:

(a) As discrete crystals with anhedral though somewhat rounded outlines which include portions of the matrix

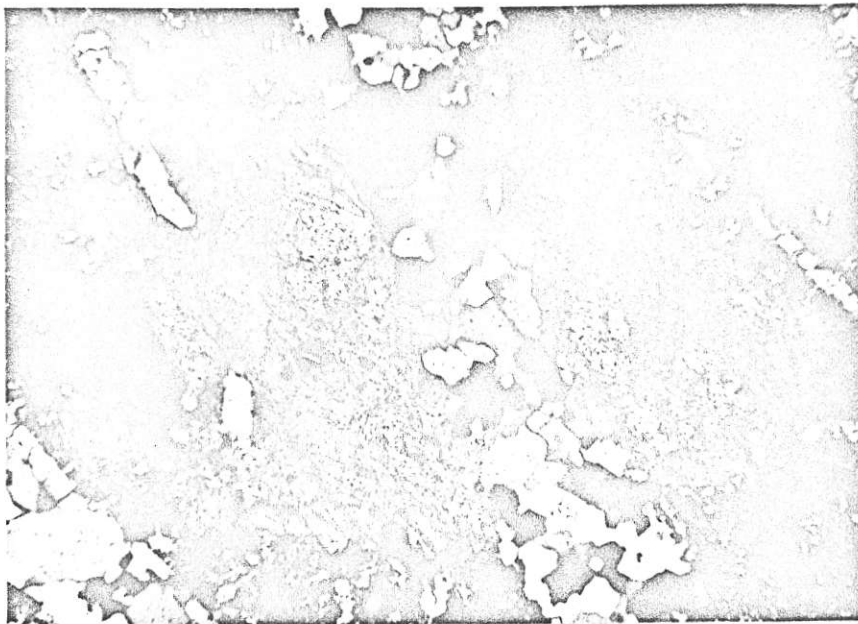
(b) As a replacement of plagioclase phenocrysts (see plates 10 and 11). The degree of replacement is variable even within a single thin-section. The highest intensity observed occurs in thin-sections L.S.-33 and T-14 where the replacement of plagioclase by potash feldspar appears as replacement microperthite (see plate 11). Chemical analyses of specimens corresponding to these two thin-sections indicate a very marked increase in  $K_2O$  and a decrease in  $Na_2O$  and  $CaO$  (see analyses 10, 11, Table V).

The absence of "grid" twinning, characteristic of microcline, suggests that the potash feldspar is orthoclase.

(iii) Argillization

Argillization also appears to be restricted to the south part of the complex. It is related to both barren and mineralized quartz-veinlets. This spatial relationship to quartz-veining is best observed in drill-holes 1 and 2. The amount of clay minerals increases towards zones of high quartz-veining in the grey biotite-quartz-feldspar and possibly in veined sections of the white quartz-feldspar porphyry. Its megascopic recognition is by the characteristic "clay" odor and the occurrence of soft, green pseudomorphs after the plagioclase phenocrysts.

In the white quartz-feldspar porphyry, the pseudomorphs are a light green color. Approximately 10 of these pseudomorphs were picked out with a needle and formed into a rolling for the X-ray powder camera. After accounting for



X 70, crossed nicols

Photomicrograph of plagioclase (white) phenocrysts indicating extensive replacement by orthoclase (grey). Albite twinning in the plagioclase is shown by alternating light grey and white bands running from top left corner to lower right corner. Taken from thin-section L.S.-38, outcrop.

Plate 10 - Potash feldspar replacement of plagioclase.



X 70, crossed nicols

Photomicrograph of plagioclase (white) showing very extensive replacement by orthoclase (grey) to produce a replacement microperthite. Taken from thin-section L.S.-38, outcrop.

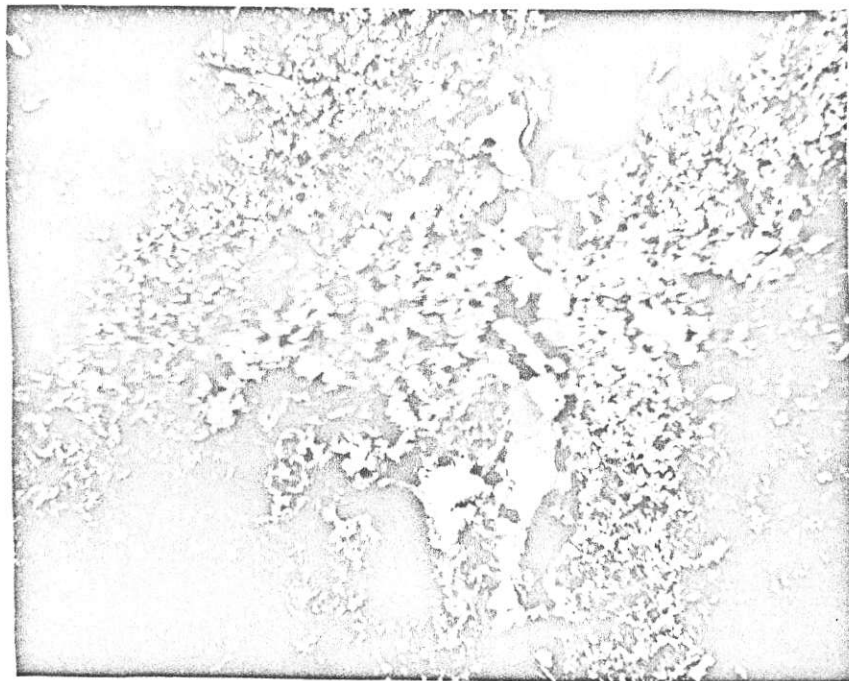
Plate 11 - Potash feldspar replacement of plagioclase.

the d-spacings due to albite, the remaining d-spacings and their intensities match either muscovite, illite, or hydro-mica (see appendix, page 84, specimen from drill-core, footage 884).

In thin-sections, the pseudomorphs appear as an aggregate of 0.1 to 0.2 mm colorless micaceous flakes replacing the plagioclase. Similar flakes border quartz veinlets (see plate 12). Their maximum interference color is first order grey, the index of refraction slightly greater than quartz. Because the flakes lack the strong birefringence generally characteristic of sericite (that is, fine-grained muscovite or paragonite), it is believed that they are illite or hydromuscovite.

In the grey biotite-quartz-feldspar porphyry, the pseudomorphs are a dark olive green. In thin-section (see plate 13), under plane polarized light, they appear as a very light green aggregate of fine-grained (< 0.05 mm), ill-defined flakes. The flakes have maximum interference colors of first order grey to yellow.

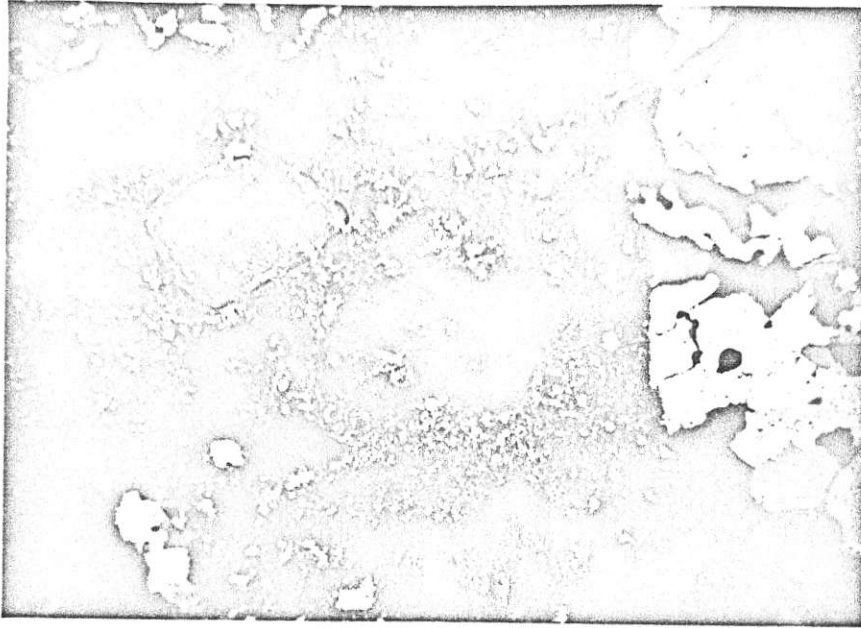
The d-spacings and relative intensities obtained from a single x-ray powder picture from these pseudomorphs are given in the appendix on page 85 (specimen from drill-hole 1, footage 671). Approximately 5 altered phenocrysts were picked



X 30, crossed nicols

Photomicrograph of illite (?) or hydro-muscovite (?) (white flakes) bordering quartz veinlets in white quartz-feldspar porphyry. Taken from thin-section of drill-core, hole 1, footage 884.

Plate 12 - Argillization of white quartz-feldspar porphyry.



X 30, crossed nicols

Photomicrograph of montmorillonite-hydromuscovite-kaolinite pseudomorphs after plagioclase. From thin-section of drill-core, hole 1, footage 671.

Plate 13 - Argillization of plagioclase phenocrysts in grey biotite-quartz-feldspar porphyry.

out with a needle and formed into a rolling for the x-ray powder camera. The pattern obtained indicates a combination of montmorillonite, hydromuscovite, and kaolinite. Montmorillonite appears to be the most abundant.

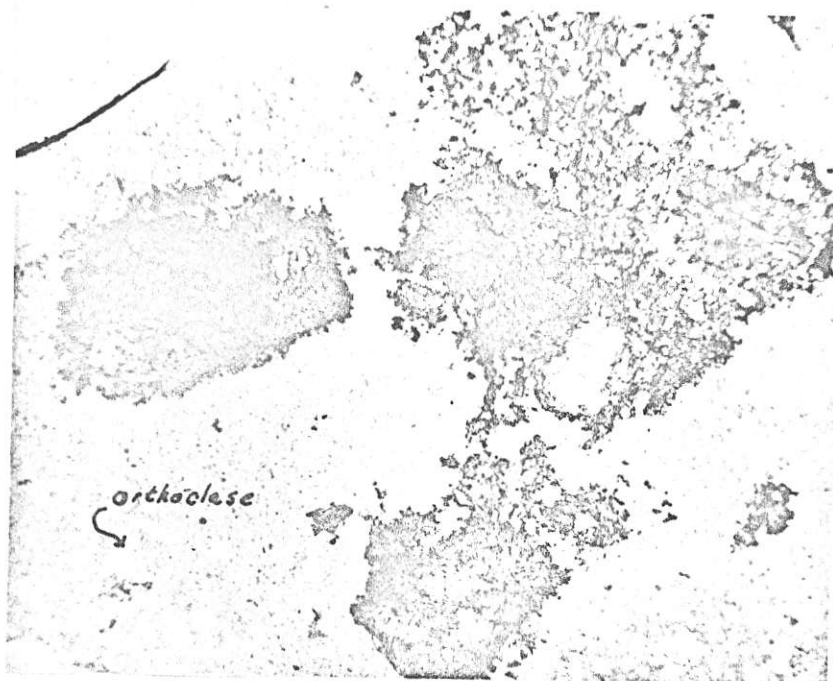
(iv) Saussuritization

Intense saussuritization of the plagioclase phenocrysts in the <sup>white</sup> quartz-feldspar porphyry occurs in the north part of the complex, east of the small pond (about specimen L.S.-56). In thin-section (see plate 14), this type of alteration is observed as pseudomorphs of epidote, calcite, and sericite after plagioclase. The presence of epidote is confirmed by an x-ray powder pattern (see appendix page 26). The distribution and significance of this type of alteration is not known completely. It does not appear in the white quartz-feldspar porphyry south of the pond. Incipient saussuritization does occur in the grey biotite quartz-feldspar porphyry in the center of the plagioclase phenocrysts. The alteration in this rock type may be due to deuteric processes, not hydrothermal effects.

(v) Pyritization

Intense pyritization occurs in the sedimentary rocks immediately adjacent to the contacts with the white quartz-feldspar porphyry and the alaskite dykes, and in parts of the white quartz-feldspar porphyry containing inclusions. In the





X 20, uncrossed nicols

Photomicrograph of epidote-calcite-sericite pseudomorphs from the alteration of plagioclase phenocrysts. An orthoclase phenocryst is in the lower left corner. Taken from thin-section L.S.-56, outcrop.

Plate 14 - Saussuritization of plagioclase phenocrysts in white quartz-feldspar porphyry.

sedimentary rocks, the pyrite occurs as disseminated crystals and as one-eighth to one-quarter inch seams along fractures. The pyrite in the white quartz-feldspar porphyry appears to bear a direct relationship to the presence of sedimentary inclusions (see fig. 4). Where there are abundant inclusions in the porphyry, the pyrite content reaches an estimated 5 per cent by volume. Where there are no inclusions, the pyrite is absent or present only in trace amounts.

Very minor amounts (less than 0.5 per cent by volume) of pyrite are associated with the molybdenite in the quartz veinlets. Drill core intersections, particularly those in the lower parts of holes 1, 2, and 3, indicate there is no defined pyrite halo about the molybdenite mineralization.

In addition to these typical hydrothermal alteration minerals, the selenite variety of gypsum and the zeolite stilbite were found in drill-hole 1. Both are found in fractures. Selenite was found only in the white quartz-feldspar porphyry. Its determination is confirmed by an x-ray powder pattern (see appendix, page 87). Stilbite occurs in the grey biotite-quartz-feldspar porphyry as milky grey, prismatic crystals in fractures. Its identification is confirmed by an x-ray powder pattern (see appendix, page 88). Neither of these minerals occur in abundance.

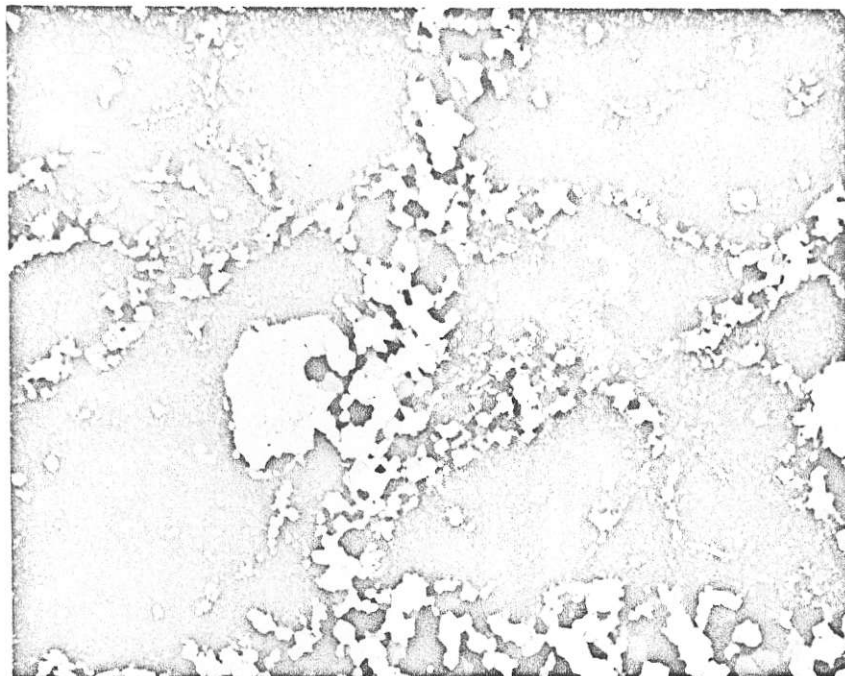
The alteration of biotite to chlorite is commonly

observed in the grey biotite-quartz-feldspar porphyry.

It is doubtful that silicification in the strict sense has taken place. All quartz veinlets observed in thin-section show very sharp contacts with the host rocks into which they have intruded (see plate 15).

The alteration types described above are exceedingly complex and somewhat ill-defined as to distribution. No definition of a zonal pattern can be made in view of the present knowledge. For example, it is not uncommon to find potash feldspathization, argillization, and sericitization in a single thin-section from the southern parts of the white quartz-feldspar porphyry. Similarly, in the northern part, the intense saussuritization is accompanied by intense sericitization. Only the argillization has a definite distribution: clay minerals bear a close spatial relationship to both mineralized and barren quartz veinlets.

Intense potash metasomatism appears to be a significant alteration process, particularly in the white quartz-feldspar porphyry and alaskite. Every thin-section of these two rock types contains some development of sericite or potash feldspar resulting from alteration. The intensities of these two alteration minerals varies; sericite is most abundant along the peripheries and in the inclusion-rich portions of the white quartz-feldspar porphyry whereas



X 16, crossed nicols

Photomicrograph of quartz veinlets cutting white quartz-feldspar porphyry. Taken from thin-section L.S.-12, outcrop.

Plate 15 - Abundant quartz veins in white quartz-feldspar porphyry.

potash feldspar appears to be restricted to the southern part of the complex. The potash feldspar may be closely related spatially to mineralization, because its abundance increases in mineralized portions. It may have preceeded mineralization however, as indicated by quartz-molybdenite veinlets that cut cleanly through the replaced plagioclase phenocrysts (see plates 10 and 11).

The formation of abundant amounts of pyrite appears to be more closely related to the presence of sedimentary rocks and inclusions derived from the sedimentary rocks, rather than to the molybdenite mineralization.

## CHAPTER V - INTERPRETATIONS AND CONCLUSIONS

Three main points of contention concerning the interpretation of the Lucky Ship Property have been:

- (i) The environment of the emplacement of the igneous rocks of the complex, in particular, the white quartz-feldspar porphyry.
- (ii) The relative ages of the white quartz-feldspar porphyry and the grey biotite-quartz-feldspar porphyry.
- (iii) The most likely igneous rock type responsible for molybdenite mineralization.

In view of the preceding descriptive chapters, the writer makes the following interpretations.

### Environment of the Igneous Rock Types

Prior to the field-mapping done in 1964, it was suggested that the white quartz-feldspar porphyry may be extrusive in its emplacement. The evidence used to support this concept was:

- (a) The fine-grained, "rhyolitic" appearance.
- (b) The apparent lack of defined intrusive contacts.
- (c) The observation in thin-sections of "flow structures" in some of the portions containing inclusions.

Data presented in the foregoing chapters indicate an

intrusive origin for the white quartz-feldspar porphyry because of:

(a) The recognition of intrusive contacts and offshoot dykes.

(b) The development of a weak thermal metamorphic halo of biotite hornfels in the sedimentary rocks adjacent to all the igneous rock types of the complex.

(c) The optical properties of the plagioclase phenocrysts imply plutonic conditions for the crystallization of white quartz-feldspar porphyry. Their  $2V_z$  values correspond to albite which has crystallized under plutonic conditions (see Table III and fig. 11).

(d) The parts of the white quartz-feldspar porphyry with inclusions display features characteristic of intrusive brecciation processes rather than an explosive volcanic formation. Both Gates (1959) and Bryner (1961) in describing breccias formed by volcanic or collapse mechanisms imply such breccias are generally pipe-like or concentric in form.

In the brecciated portions of white quartz-feldspar porphyry on the Lucky Ship Property, the breccia as known is extremely irregular in form and distribution. There is no intense shattering or jointing marking the peripheries. Jointing appears to be equal in intensity in both brecciated and non-brecciated portions. The number of fragments does

not decrease sharply towards non-brecciated portions; the change appears gradational. The brecciated portions thus best fit the description of the formation of non-effusive breccias given by Bryner (1961):

"...A magma, in the process of intrusion, may entrain enough solid material to form a breccia. This material can be derived by magmatic stoping, by abrasion of wallrocks, if the magma is viscous, or by engulfment of other breccias. An intrusive breccia also can originate where a chilled border or front is brecciated and then inundated by a surge of underlying magma....."

The above process of formation is thought to be the case for the formation of the brecciated portions present in the white quartz-feldspar porphyry on the Lucky Ship Property. Thus the breccia now appears as angular fragments of argillite-greywacke, fragments of the dark green aphanitic dykes, and white quartz-feldspar porphyry fragments, held in a matrix of white quartz-feldspar porphyry. The presence of white quartz-feldspar porphyry fragments surrounded by white quartz-feldspar porphyry matrix implies the brecciation occurred during the crystallization of the white quartz-feldspar porphyry magma. Most significantly, the brecciation is intramineralization. This is indicated by brecciated portions seen in core from drill-hole 4 and in outcrops where fragments are mineralized and both matrix and fragments are in turn cut by quartz-molybdenite veinlets.



The Relative Ages of White Quartz-Feldspar  
Porphyry and Grey Biotite-Quartz-Feldspar Porphyry,  
and the Genesis of Molybdenite Mineralization

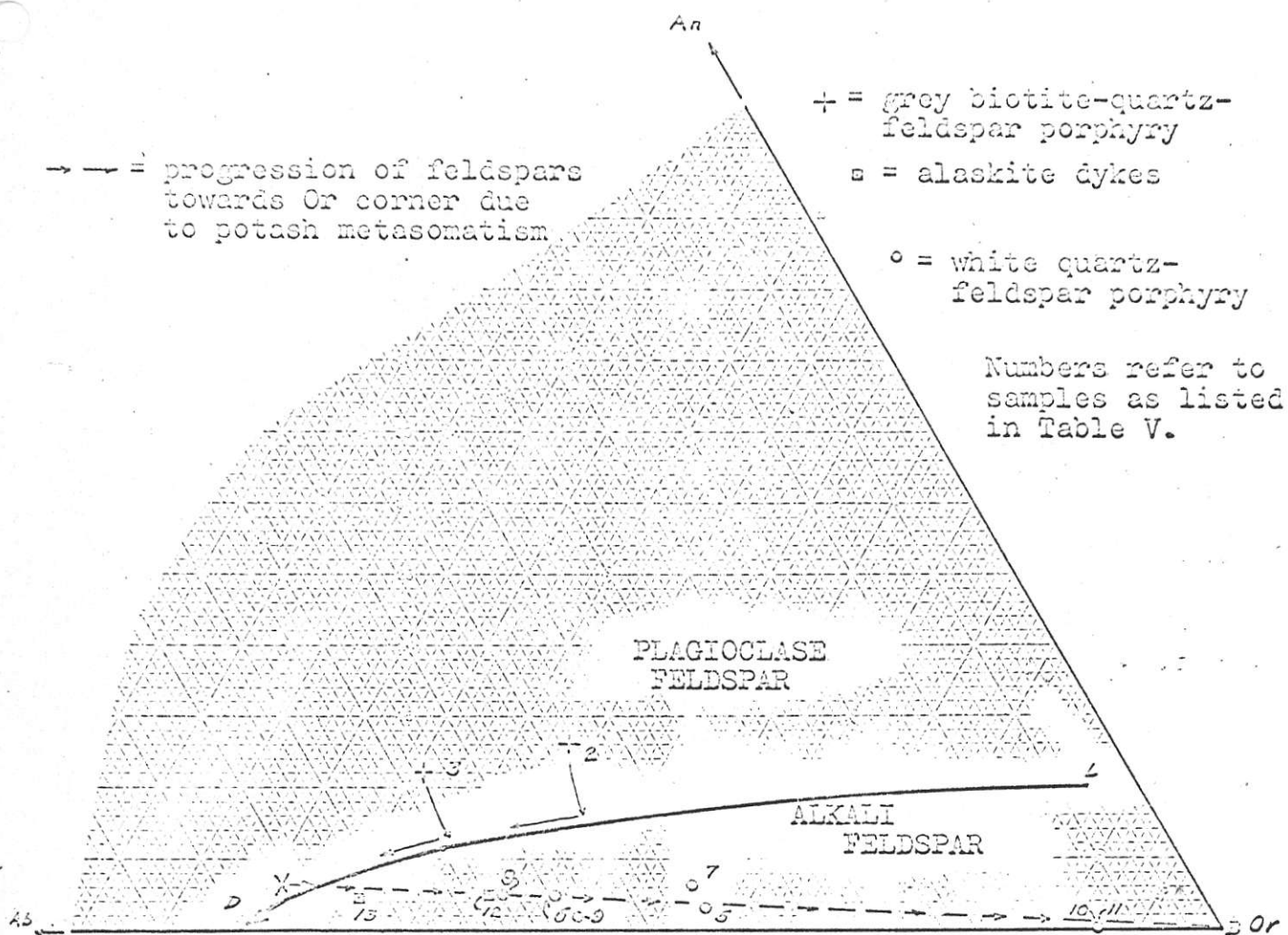
In the foregoing descriptive chapters it has been shown that the grey biotite-quartz-feldspar porphyry and the white quartz-feldspar porphyry differ in their mineralogy and geochemistry. The alaskite dykes are similar and thus are believed to have a genetic relationship to the white quartz-feldspar porphyry. A genetic relationship of the white quartz-feldspar porphyry to the grey biotite-quartz-feldspar porphyry is indicated by the following chemical and textural relationships.

In thin-sections of the white quartz-feldspar porphyry it appears that the plagioclase phenocrysts are earlier in the sequence of crystallization than the primary potash feldspars. If the normative minerals, albite, anorthite, and orthoclase feldspar are plotted (see fig. 14) on the schematic crystallization system of albite-anorthite-orthoclase (Barth, 1962), it is seen that the potash feldspar should have crystallized first, not plagioclase, thus conflicting with the thin-section interpretation.

The normative feldspars for both the alaskite and

the white quartz-feldspar porphyry in fig. 14 plot on a line, with the most altered rocks closest to the orthoclase corner, thus indicating a relative increase in  $K_2O$  and a decrease in  $Na_2O$  and  $CaO$ . In the opposite direction, the normative feldspars progress towards the boundary line L-D. It is conceivable that the position of the normative feldspars representing the primary composition of the melt is on the plagioclase side of the boundary line in the vicinity of X, thus explaining the sequence interpreted from thin-sections. Potash metasomatism, represented by sericite and potash feldspar as alteration minerals, has resulted in normative plots in the alkali feldspar field.

In the crystallization of grey biotite-quartz-feldspar porphyry, the plagioclase phenocrysts would have crystallized first, followed by simultaneous crystallization of plagioclase and potash feldspar. In thin-section, the crystallization sequence appears in this manner. During crystallization, the melt composition would have progressed from the compositions plotted as + (plots 2 and 3) to the boundary line L-D and then along the boundary line towards D. Presumably in the later stages of crystallization, the melt could have attained the composition corresponding to that postulated for the primary composition of the white quartz-feldspar porphyry at point X. Thus a melt responsible



→ = progression of feldspars towards Or corner due to potash metasomatism

+ = grey biotite-quartz-feldspar porphyry

■ = alaskite dykes

○ = white quartz-feldspar porphyry

Numbers refer to samples as listed in Table V.

X = proposed primary composition of white quartz-feldspar porphyry and alaskite dykes.

L-D = boundary line marking the simultaneous crystallization of plagioclase feldspar and alkali feldspar, and separating the fields of plagioclase feldspar and alkali feldspar.

Fig. 14 - Schematic crystallization of the System Albite-Anorthite-Orthoclase showing the derivation of white quartz-feldspar porphyry from grey biotite-quartz-feldspar porphyry (after Barth, 1962).

for the white quartz-feldspar porphyry showing the albitic plagioclase phenocrysts to be earlier than the potash feldspar may have been derived from the late stage melt of the grey biotite-quartz-feldspar porphyry.

The writer believes that in the elevations from surface to the depths tested by diamond drilling, these two rock types bear an intrusive relationship to one another. This is indicated by drill-core which shows that the two rock types have cross-cutting relationships. However, where mutual contacts likely exist (for instance in drill-holes 1, 2, and 3), the actual contact is masked by intense quartz veining and alteration, thus making it impossible to assign relative ages on the basis of contact relationships. Therefore, the writer believes the following features are significant in interpreting the relative ages of these two rock types.

(a) In a general aspect, based solely on outcrop observations, it appears that the molybdenite mineralization is arranged about the grey biotite-quartz-feldspar porphyry. A more detailed knowledge of the distribution of molybdenite, obtained from drill-core, indicates that the white quartz-feldspar porphyry and the alaskite dykes contain the best mineralization.

(b) Drill-core indicates that the grey biotite-quartz-feldspar porphyry is often separated from the white

quartz-feldspar porphyry by sedimentary rocks. Furthermore, these sedimentary rock intersections (in particular, see the central footages of drill-hole 3) are relatively poor in molybdenite mineralization.

(c) Some molybdenite mineralization is associated with the white quartz-feldspar porphyry. This is indicated by the occurrence of mineralized fragments in this rock type. Both the fragments and the surrounding rock are in turn cut by a second period of mineralization.

(d) The dark green, aphanitic dykes have been found cutting only sedimentary rocks and the grey biotite-quartz-feldspar porphyry rock. What appears to be fragments of the dykes have been found in the white quartz-feldspar porphyry.

Two different sequences of intrusion and mineralization can be derived from the above features:

(i) White quartz-feldspar porphyry, followed by grey biotite-quartz-feldspar porphyry and the molybdenite mineralization.

(ii) Grey biotite-quartz-feldspar porphyry followed by white quartz-feldspar porphyry and the molybdenite mineralization.

The first of the above sequences is indicated only by the vague suggestion in outcrop that molybdenite mineralization occurs peripherally to the grey biotite-quartz-feldspar porphyry. This peripheral arrangement suggests that

the intrusion of this rock type provided the shattering mechanism and that the mineralization was derived from its late hydrothermal solutions. Since there is molybdenite in the white quartz-feldspar porphyry, this body of rock would have preceded the emplacement of the grey biotite-quartz-feldspar.

The writer believes that the above features (a, b, c, d) indicate the second sequence happened; the grey biotite-quartz-feldspar porphyry preceded the white quartz-feldspar porphyry and the molybdenite mineralization. The reasons for this belief are as follows.

(i) The presence of dark green aphanitic dykes in the grey biotite-quartz-feldspar porphyry and their absence, except as inclusions, in the white quartz-feldspar porphyry, suggests a sequence of:

- (1) Grey biotite-quartz-feldspar porphyry  
(earliest).
- (2) Dark green aphanitic dykes.
- (3) White quartz-feldspar porphyry (latest).

(ii) The distribution of the highest grades of molybdenite mineralization is closely associated with the distribution of the white quartz-feldspar porphyry and the alaskite dykes, not with the distribution of the grey biotite-quartz-feldspar porphyry. This feature is clearly indicated in the core from drill-hole 2. Furthermore, mineralized

fragments occur in the white quartz-feldspar porphyry. The porphyry and the fragments are in turn cut by a second period of molybdenite mineralization. Therefore, the writer believes that these features indicate some, if not all, of the mineralization is associated with the crystallization history of this rock type. Since there is minor quartz-molybdenite veinlets in the grey biotite-quartz-feldspar porphyry, this rock type was in place before mineralization and therefore before the white quartz-feldspar porphyry.

(iii) If there is a genetic relationship (see fig. 14) between these two rock types, then the white quartz-feldspar porphyry is the last rock in the sequence because it was presumably derived from the late stage melt portion of the grey biotite-quartz-feldspar porphyry.

In summary, the writer believes that the white quartz-feldspar porphyry was the last rock to be emplaced. The molybdenite mineralization is believed to be tied in closely with the crystallization of this rock type, in keeping with the genetic concepts pointed out by Vokes (1963):

"The close association of deposits of the pegmatitic, pegmatitic-quartz vein, and quartz-vein types with igneous intrusions, particularly acid intrusions, is strong evidence for regarding that the two have a common origin. The metal appears to have concentrated in the last crystallizing fractions of the intrusions, with the deposits forming at or near the margins of the igneous bodies."

Conclusions

(i) The igneous rocks of the Lucky Ship Complex are intrusive and were emplaced in a shallow environment.

(ii) The white quartz-feldspar porphyry and the alaskite dykes are related. This is indicated by similar plagioclase and bulk chemical compositions.

(iii) An intrusive sequence, from oldest to youngest, is suggested as: (a) grey biotite-quartz-feldspar porphyry (b) dark green aphanitic dykes (c) white quartz-feldspar porphyry and alaskite dykes. The position of the pink quartz porphyry is unknown due to the lack of knowledge of contact relations.

(iv) It is probable that the alaskite dykes and the white quartz-feldspar porphyry are genetically related to the grey biotite-quartz-feldspar porphyry; their magma(s) being derived from the latter's late stage liquid portion. This derivation presumably could have taken place at a deeper level than present observations by a process of "filter pressing". This concept is based on the fact that chemical analyses of the alaskite and the white quartz-feldspar porphyry give normative feldspar plots which trend in a manner contradictory to the observed crystallization sequence when considered in view of the crystallization system of albite-anorthite-orthoclase. Potash metasomatism, represented mineralogically by sericite and replacement potash feldspar, and chemically



by a linear trend of the normative feldspars towards the orthoclase corner of the feldspar phase diagram, is interpreted to be the cause of this contradiction.

(v) White quartz-feldspar porphyry has undergone a complex intrusive history. It is suggested that the emplacement has been repetitive, marked by the breaking and the alteration of partially crystallized portions and the sedimentary wall-rocks. This complexity is amply demonstrated by the number and types of inclusions present in parts of this rock type.

(vi) The molybdenite mineralization is associated with the crystallization history of the alaskite dykes and the white quartz-feldspar porphyry. This is indicated by the mineralized fragments in the brecciated portions and the close spatial relationship of the highest grades of mineralization to these two rock types.

(vii) Argillization is associated with quartz veining and mineralization. Mineralizing solutions are interpreted as being hydrothermal in nature, derived from late stage differentiates of the alaskite and the white quartz-feldspar porphyry. The potash feldspar developed by replacement processes may be closely related but prior to molybdenite mineralization.

REFERENCES

- Armstrong, J. E., 1944, Preliminary Map, Smithers, British Columbia; Geol. Surv., Canada, Paper 44-23.
- Barth, T. F. W., 1962, Theoretical Petrology; John Wiley and Sons Inc., Second Edition, pp. 36 to 39.
- British Columbia; Minister of Mines Annual Reports, 1957, pp. 13.
- Bryner, L., 1961, Breccia and Pebble Columns Associated With Epigenetic Ore Deposits; Economic Geology, Vol. 56, No. 3, pp. 488 to 503.
- Chayes, F., 1949, A Simple Point Counter for Thin-section Analysis; American Mineralogist, Vol. 34, pp. 151 to 168.
- Deer, W. A., Howie, R. A., and Zussman, 1962, Rock Forming Minerals; Vol. 3, Sheet Silicates, Longman's Canadian Ltd.
- Duffel, S., 1959, Whitesail Lake Map-Area; Geol. Surv., Canada, Mem. 299, pp. 35 to 46, 55 to 64.
- Duffel, S. and Souther, J. G., 1964, Geology of Terrace Map-Area, British Columbia; Geol. Surv., Canada, Mem. 329, pp. 21 to 27, 33 to 68.
- Emmons, R. C., 1943, The Universal Stage (With Five Axes of Rotation); Geol. Soc. of America, Memoir 8, pp 151 to 168.
- Gates, O., 1959, Breccia Pipes in the Shoshone Range, Nevada; Economic Geology, Vol. 54, No. 5, pp. 790 to 815.
- Lang, A. H., 1942, Houston Map-Area; Geol. Surv., Canada, Map 671 A, 1942.
- Nockolds, S. R., 1954, Average Chemical Compositions of Some Igneous Rocks; Bull. of Geol. Soc. of America, Vol. 65, pp. 1007 to 1032.
- Rice, H. M. A., 1949, Smithers-Port St. James Area, British Columbia; Geol. Surv., Canada, Map 971 A.
- Schwartz, G. M., 1955, Hydrothermal Alteration as a Guide to Ore; Economic Geology, Fiftieth Anniversary Volume, Part I, pp. 300 to 323.

- Slemmons, D. B., 1962, Determination of Volcanic and Plutonic Plagioclases Using a Three-or -Four-Axis Universal Stage; Geol. Soc. of America, Special Paper 69.
- Turner, F. J. and Verhoogen, J., 1951, Igneous and Metamorphic Petrology; McGraw-Hill Book Company, Inc., Second Edition, pp. 251.
- Tyrell, G. W., 1926, The Principles of Petrology; E. P. Dutton and Company Inc., pp. 113.
- Vokes, F. M., 1963, Molybdenum Deposits of Canada; Geol. Surv., Canada, Economic Geology Report N. 20, pp. 53, 54.

APPENDIX

X-Ray Powder Picture Data For

Albite-Illite-Muscovite-Hydromuscovite  
Montmorillonite-Hydromuscovite-Kaolinite

Epidote

Gypsum

Stilbite

Altered Plagioclase		Albite ASTM 9-466		Illite ASTM 9-334		Muscovite ASTM 7-42		Hydromuscovite ASTM 2-0462	
I	dA°	I	dA°	I	dA°	I	dA°	I	dA°
30	10.009			80	9.9	80	9.9	80	10.00
10	6.363	20	6.39						
		1	5.94						
		1	5.59						
10	4.39			60	4.9	53	4.99	80	5.03
30	4.506			100	4.46	19	4.46	60	4.52
				40	4.29				
				40	4.11				
30	4.038	15	4.03						
10	3.340	7	3.85	60	3.88	10	3.87		
20	3.77	25	3.73						
30	3.663	20	3.684	50	3.65	8	3.60	80	3.63
		15	3.663						
		10	3.509						
		1	3.484						
		1	3.375						
50	3.339			100	3.36	100	3.33	100	3.35
100	3.139	100	3.196						
		9	3.151	50	3.10	10	3.11	80	3.10
10	2.973	9	2.964						
10	2.921	15	2.933					80	2.90
		7	2.866	60	2.86	16	2.83		
		1	2.843						
		1	2.787						
		5	2.639			15	2.60		
60	2.576	7	2.563	100	2.57	27	2.57	100	2.60
		1	2.538						
		1	2.51			5	2.50		
		5	2.496						
10	2.447	5	2.460	50	2.45	7	2.45	60	2.47
10	2.394			60	2.39	8	2.38	80	2.39
		+ weak		50	2.24			40	2.27
		lines		60	2.14			40	2.18
		to		60	1.992			80	2.14
		1.839		40	1.94			100	1.99
				60	1.650			20	1.72
								80	1.65
20	1.498			80	1.50			80	1.51
				+ others					
				to 1.245					

Camera Type: Circular X-ray powder camera

Size: 114.6 mm

Radiation: Fe/Mn

Comparison of intensities and d-spacings of altered plagioclase phenocrysts in white quartz-feldspar porphyry with those of ASTM index cards 9-334 (illite), 7-42 (muscovite), 9-466 (albite), and 2-0462 (hydromuscovite). The altered phenocrysts are from drill-core, hole 1, footage 334.

Altered Plagioclase		Montmorillonite ASTM 13-135		Hydromuscovite ASTM 2-0462		Kaolinite ASTM 6-0221		
I	dA°	I	dA°	I	dA°	I	dA°	
100	14.416	100	15.0					
30	10.06			80	10.00			
30	7.159					100	7.18	
10	5.019	60	5.01	80	5.03			
30	4.472 <sub>B</sub>	80	4.50	60	4.52	80	4.48	
10	3.784	20	3.77					
10	3.652			80	3.68			
20	3.572					100	3.58	
		10	3.50			80	3.56	
70	3.349			100	3.35			
		10	3.30					
30	3.189	--strongest line for plagioclase--						
				80	3.10			
10	3.042	60	3.02	80	2.90			
40	2.565 <sub>S</sub>	40	2.58	100	2.60	80	2.565	
		40	2.50	60	2.47	80	2.502	
	+ very weak lines			80	2.39	80	2.386	
		10	2.26	40	2.27	90	2.341	
				80	2.18	10	2.206	
		10	2.15	80	2.14			
10	2.002			100	1.99	40	1.939	
		10	1.88			40	1.739	
10	1.705	30	1.70	20	1.72			
				80	1.65	50	1.666	
20	1.493 <sub>S</sub>	50	1.50	80	1.51	10	1.541	
		50	1.493			100	1.488	
		20	1.285				+ lines to	
		20	1.243				1.194	

Camera type: Circular X-ray powder camera.

Size: 114.6 mm

Radiation: Fe/Mn

Comparison of intensities and d-spacings of altered plagioclase phenocrysts in grey biotite-quartz-feldspar porphyry with those of ASTM index cards 13-135 (montmorillonite), 2-0462 (hydromuscovite), and 6-0221 (kaolinite). The altered plagioclase was obtained from drill-core, hole 1, footage 671.

Altered (epidote)  
Plagioclase Phenocrysts

I	dA°
30	3.5
60	5.0
60	3.9
90	3.38
10	3.15
100	2.38
10	2.8
10	2.65
10	2.55
40	2.38
30	2.27
20	2.12
20	2.08
40	1.85
10	1.80
70	1.64
20	1.56
30	1.525
30	1.42
30	1.39
+ weak lines	

Epidote  
ASTM 9-438

I	dA°
5	7.98
3	7.02
40	5.018
1	4.621
40	3.937
1	3.762
40	3.492
7	3.372
15	3.197
1	3.060
100	2.900
50	2.809
60	2.677
55	2.533
10	2.525
7	2.449
70	2.396
25	2.289
25	2.161
40	2.11
11	2.065
1	2.043
1	2.020
1	2.003
1	1.914
60	1.869
1	1.773
1	1.742
1	1.705
1	1.687
1	1.669
65	1.635
11	1.622
11	1.590
13	1.574
7	1.539
15	1.458
7	1.435
30	1.404
25	1.389

Camera type: circular X-ray  
powder camera.

Size: 57.3 mm

Radiation: Fe/Mn

Comparison of intensities and d-spacings of epidote in altered plagioclase phenocrysts from white quartz-feldspar porphyry with those of the ASTM index card 9-438 (epidote). The epidote was obtained from specimen L.S. 56 (see fig. 7 for location, east of the pond).





Stilbite  
Lucky Ship Property

I	dA <sup>o</sup>
90	9.184
5	5.387
60	4.675
5	4.303
100	4.072
10	3.752
20	3.388
15	3.201
30	3.042
10	2.783
	+ very weak lines
5	2.05

Stilbite  
ASTM 10-433

I	dA <sup>o</sup>
90	9.1
20	5.4
70	4.63
30	4.30
100	4.08
40	3.74
50	3.41
50	3.20
70	3.03
30	2.79
20	2.69
20	2.59
30	2.26
20	2.04

Camera type: circular X-ray powder camera.

Size: 57.3 mm.

Radiation: Fe/Mn.

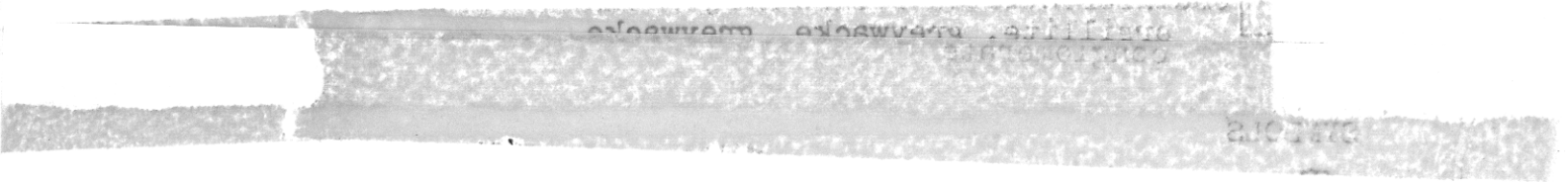
Comparison of intensities and d-spacings of stilbite from the Lucky Ship Property with those of ASTM index card 10-433. The stilbite occurs in a fracture in grey biotite-quartz-feldspar porphyry from drill core, hole 1, footage 239.

LEGEND FOR FIGURES 4, 6, and 7

To accompany M. Sc. thesis:  
Petrology and Molybdenite  
Mineralization of the Lucky  
Ship Igneous Complex.







By: D. A. Silversides

Figure 3






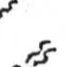
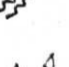










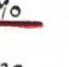


LEGEND

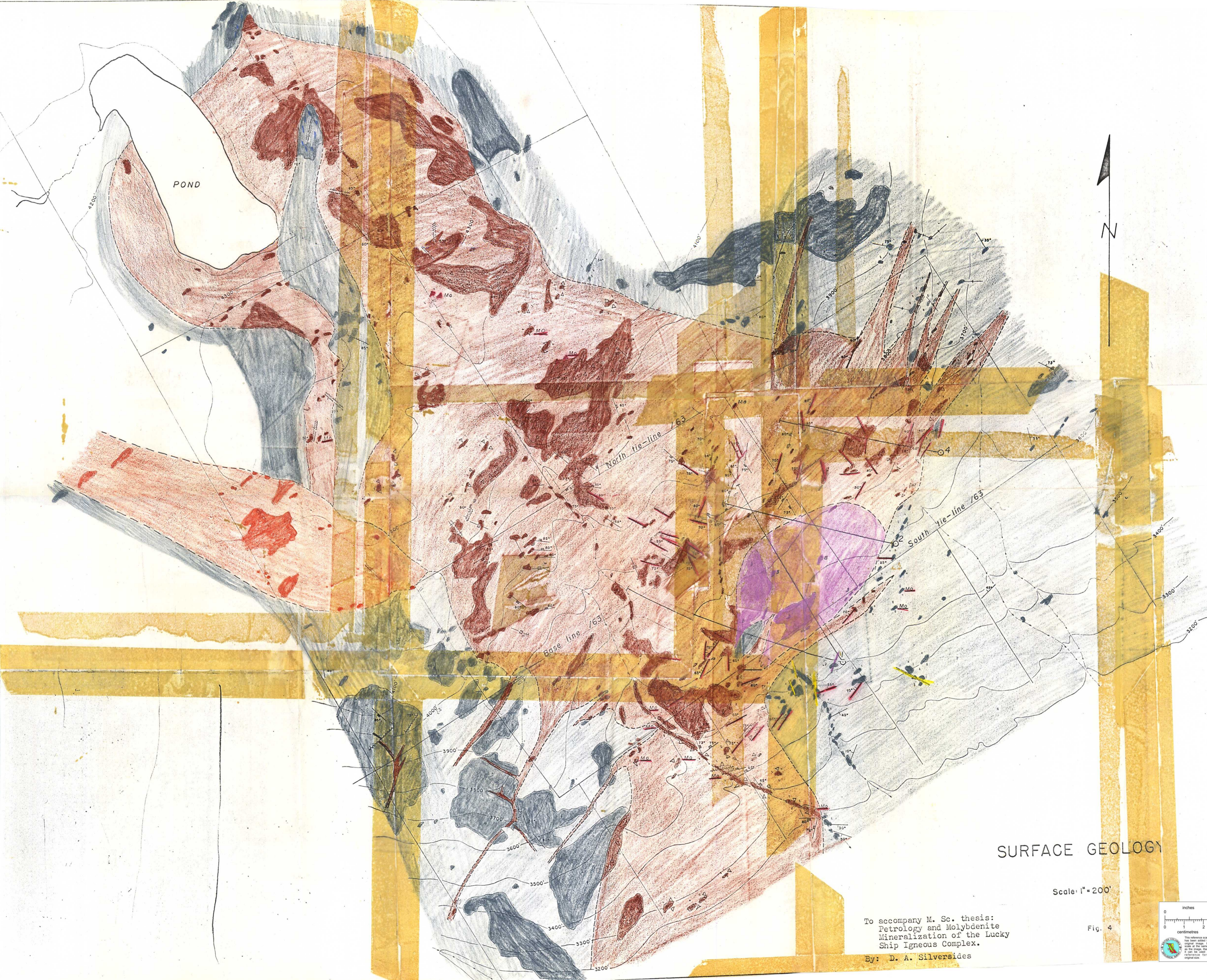
ROCK TYPES

-  Pink quartz porphyry
-  White quartz-feldspar porphyry
-  Alaskite dyke
-  Dark green aphanitic dyke
-  Grey biotite-quartz-feldspar porphyry
-  Undifferentiated sedimentary rocks:  
argillite, greywacke, greywacke  
conglomerate

SYMBOLS

-  Outcrop
-  Geologic contact: observed, assumed
-  Bedding and contact attitudes
-  Jointing attitude
-  Fault
-  Shear; closely spaced joints
-  Fragments of sedimentary and white quartz-feldspar porphyry rocks present as inclusions in white quartz-feldspar porphyry
-  1 to 5% by volume disseminated pyrite. Unstippled areas have trace to nil amounts of pyrite
-  Biotite
-  Abundant barren quartz in drill core
-  Attitude of quartz-molybdenite veinlets
-  Molybdenite-mineralized fragments of white quartz-feldspar porphyry
-  Minor molybdenite mineralization
-  Molybdenite mineralization in drill core: histogram showing number of quartz-molybdenite veinlets/10 ft. of core length
-  Diamond drill hole
-  Picket lines
-  Intermittent creek
-  Contour line



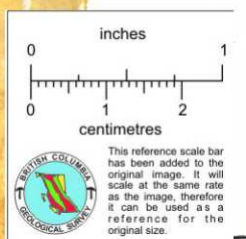


SURFACE GEOLOGY

Scale: 1" = 200'

To accompany M. Sc. thesis:  
 Petrology and Molybdenite  
 Mineralization of the Lucky  
 Ship Igneous Complex.  
 By: D. A. Silversides

Fig. 4





ELEVATION  
3800'

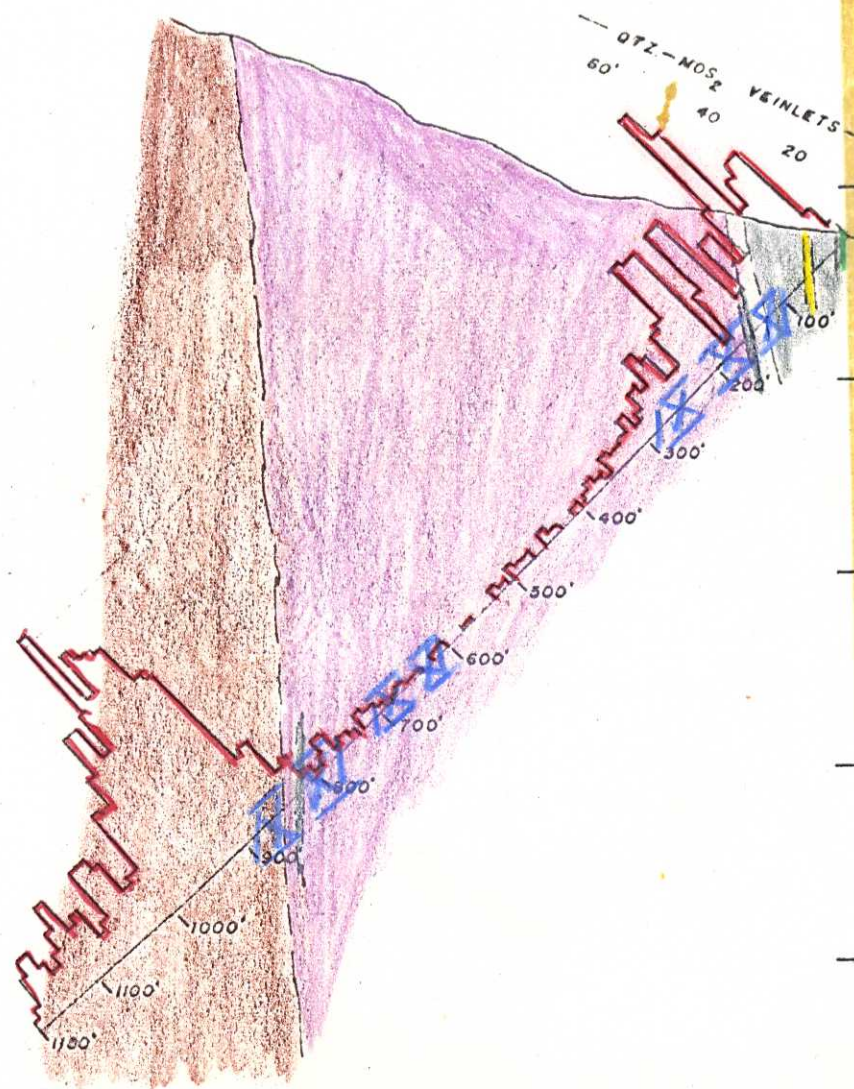
3600'

3400'

3200'

3000'

2800'



DRILL-HOLE 1

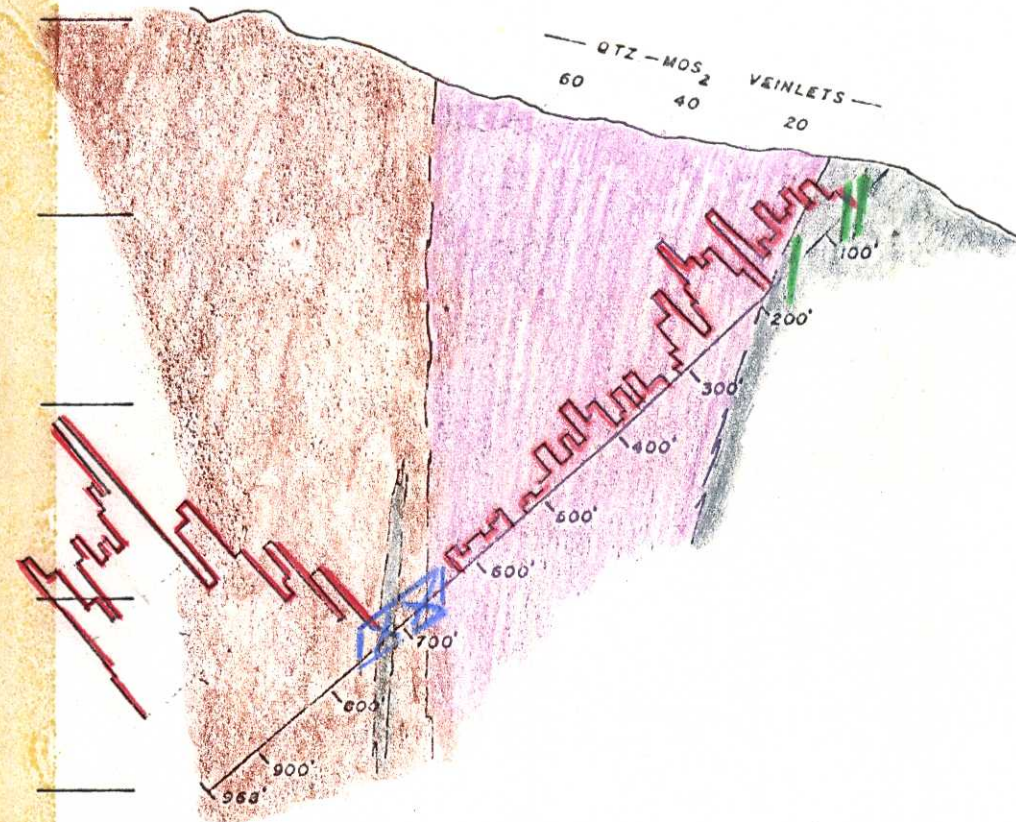
ELEVATION  
3800'

3600'

3400'

3200'

3000'



DRILL-HOLE 2

DRILL-HOLE 3

DRILL-HOLE 4

ELEVATION

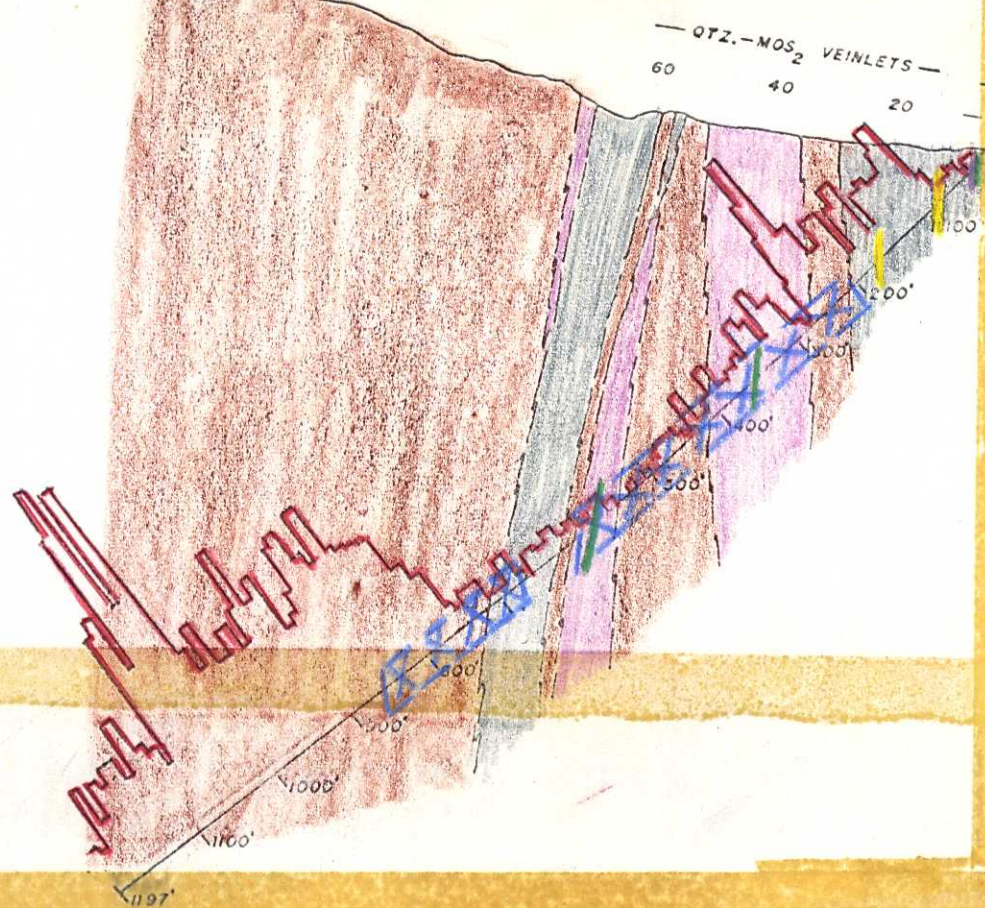
3600'

3400'

3200'

3000'

2800'



ELEVATION

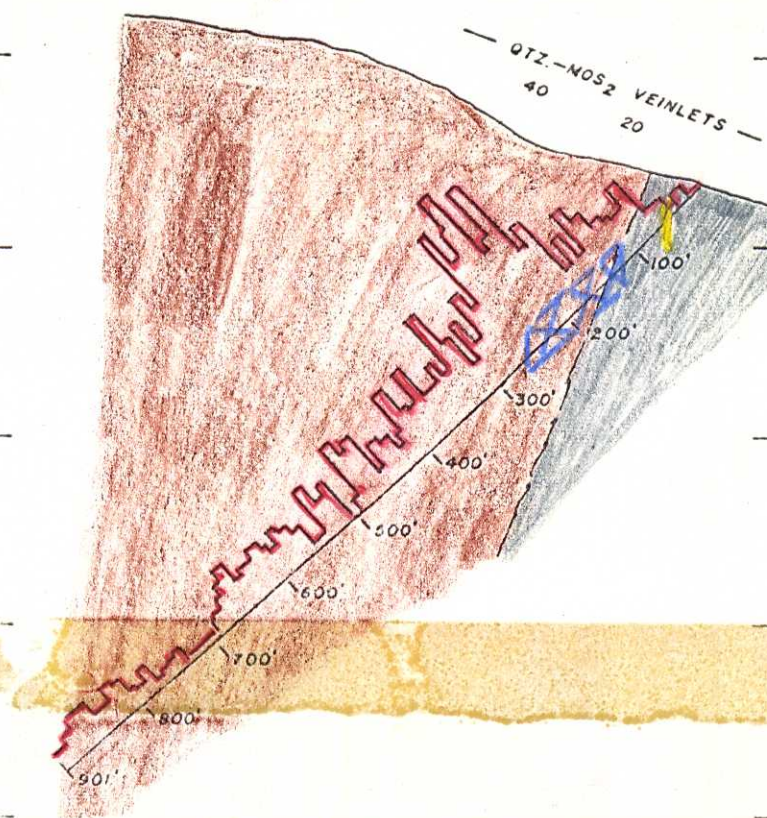
3800'

3600'

3400'

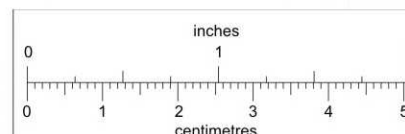
3200'

3000'



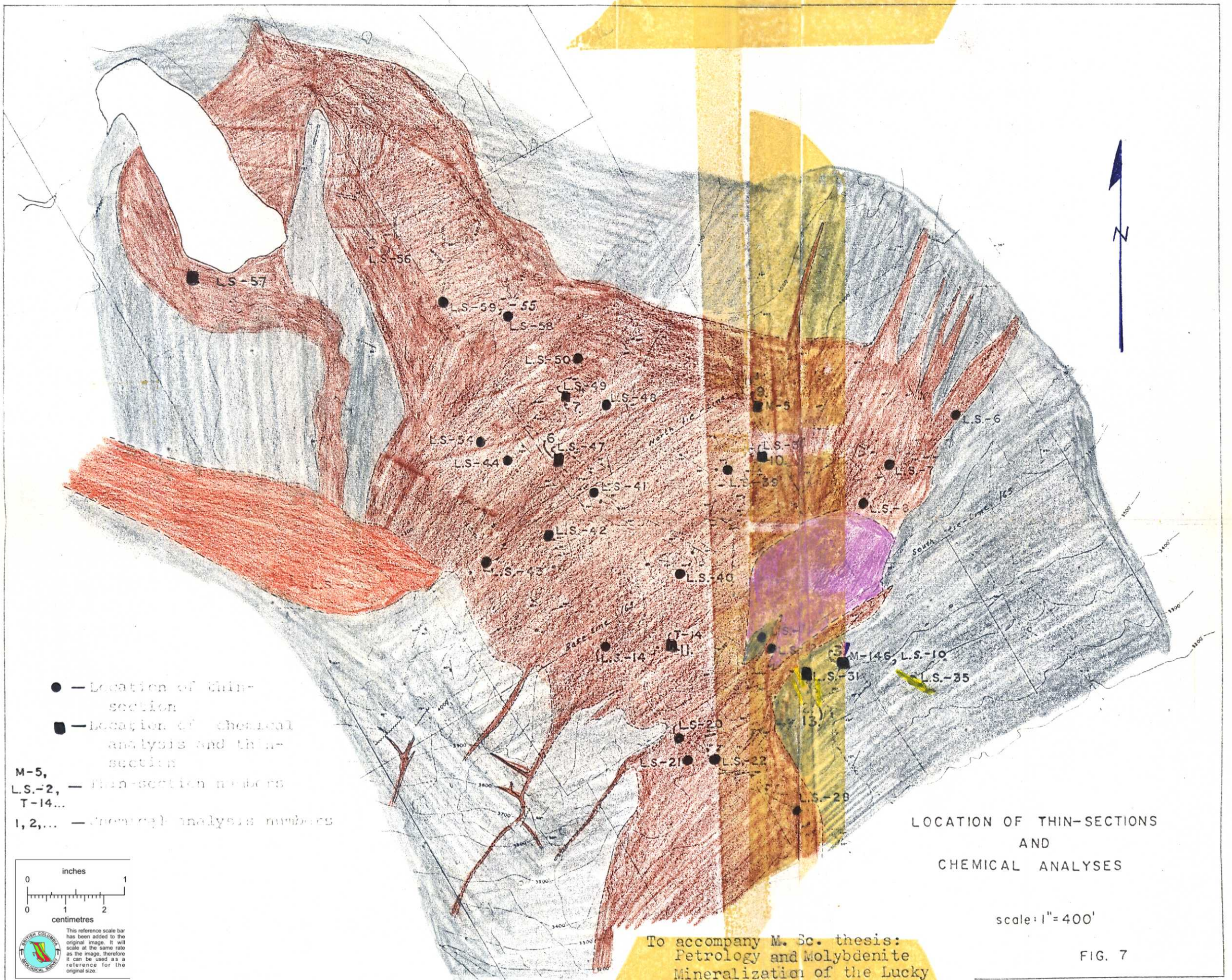
DIAMOND DRILL-HOLE  
CORRELATIONS

All drill-holes viewed looking northeast



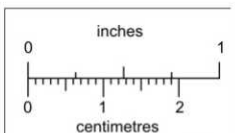
This reference scale bar has been added to the original image. It will scale at the same rate as the image, therefore it can be used as a reference for the original size.





- — Location of thin-section
- — Location of chemical analysis and thin-section

M-5,  
L.S.-2, — thin-section numbers  
T-14...  
1, 2, ... — chemical analysis numbers



This reference scale bar has been added to the original image. It will scale at the same rate as the image, therefore it can be used as a reference for the original size.

LOCATION OF THIN-SECTIONS AND CHEMICAL ANALYSES

scale: 1" = 400'

To accompany M. Sc. thesis:  
Petrology and Molybdenite  
Mineralization of the Lucky  
Ship Igneous Complex.

By: D. A. Silversides

FIG. 7